Tropical Disturbance Intensification

By
Raymond Zehr

Department of Atmospheric Science
Colorado State University
Fort Collins, Colorado

Colorado State University

Department of
Atmospheric Science

Paper No. 259

TROPICAL DISTURBANCE INTENSIFICATION

By

Raymond Zehr

Department of Atmospheric Science

Colorado State University

Fort Collins, Colorado

December, 1976

Atmospheric Science Paper No. 259

ABSTRACT

An observational study of tropical cyclone genesis was made by compositing western Pacific rawinsonde data with respect to both pre-typhoon and non-developing cloud clusters. The size, intensity, and mean vertical motion of the disturbances which eventually evolved into typhoons were similar to the non-developing clusters which did not intensify. However, four primary physical differences between pre-typhoon and non-developing clusters are found. 1) The low-level relative vorticity with the pre-typhoon clusters was about twice as large. 2) The non-developing clusters were cold-core in the 500-800 mb layers while the pre-typhoon clusters were slightly warm-core at these levels. 3) The ventilation (non-divergent flow through the cluster area) which advects heat energy away from the cluster was larger with the non-developing clusters in the warm-core layers (200-500 mb) and ventilation of moisture out of the non-developing clusters was significantly larger at lower tropospheric levels (500-900 mb). 4) The outflow in the upper troposphere was similar in magnitude but markedly more anticyclonic with the pre-typhoon clusters.

Boundary layer (surface-900 mb) frictional convergence accounts for only a small fraction of the net mass convergence into the pre-typhoon cloud cluster which typically extends up to 300-400 mb. The percentage of boundary layer convergence to total convergence does, however, increase as the intensification process proceeds. Other physical mechanisms such as cloud cluster minus surrounding radiational differences must likely be hypothesized to explain the cloud cluster's deep-layer inflow in its early stages of existence and intensification.

1. INTRODUCTION

An average of eighty typhoons, hurricanes, and tropical storms are spawned annually over warm tropical oceans. Although these storms have been studied extensively in recent years, the formation or cyclogenesis is not well understood. It is well known that tropical cyclones form only in very warm oceanic regions (sea surface temperature > 26.5°C), which are characterized by plentiful cumulonimbus convection (Palmén, 1948). It is also now generally accepted that tropical storm genesis occurs in regions of relatively small vertical wind shear, (Gray, 1968, 1975).

In tropical regions, the most prevalent synoptic scale weather systems are cloud clusters. These systems have very weak surface pressure and wind patterns, propagate westward at 4-8° longitude per day, and have an average diameter of 3-8° latitude. They are easily identified from satellite pictures but are highly variable in size and shape. Cloud clusters are characterized by active cumulonimbus convection and extensive cirrus cloud shields. Williams and Gray (1973) and Ruprecht and Gray (1976) have established the basic features of these systems by compositing numerous rawinsonde observations within the clusters. Chang (1970) and Wallace (1970) have depicted the conservative features and persistence of cloud clusters with the aid of time-longitude sections of satellite pictures. The period during which an individual cloud cluster can be identified is also highly variable, ranging from a few hours to several days.

It has been observed that typhoons originate from cloud clusters which have a general appearance similar to the non-developing clusters.

1

These pre-typhoon cloud clusters are the main subject of this investiga-
tion. Figure 1 shows DMSP (Defense Meteorological Satellite Program)
satellite pictures of eight clusters of each type, those which developed
into typhoons and those which did not intensify. All of the pre-typhoon
clusters pictured were located in or near the equatorial trough (ITCZ)
in the western Pacific and eventually developed into typhoons during
1972. The non-developing clusters shown in Fig. 1 were observed in the
same area of the western Pacific during August and September, 1972. Al-
though a careful analysis of many satellite pictures of each cluster
type may reveal differences, a single cluster can not easily be identi-
fied as a pre-typhoon disturbance from a satellite picture.

The genesis of hurricanes and typhoons has been observed to occur
predominantly in two types of low-level flow regimes. Gray (1968) iden-
tified these genesis types as Type A, which is in direct association
with the equatorial trough (ITCZ), and Type B in which the disturbance
is completely embedded in easterly trade-wind flow. Type B generally
refers to genesis poleward of about 15-18° latitude and comprises only
about 15-20% of the global total of storms. However, numerous North
Atlantic hurricanes originate from the Type B genesis. The Type A genesis
generally occurs equatorward of about 15-18° latitude and includes ap-
proximately 80-85% of the global total of storms. Sadler (1967a) con-
curs with this. He observes that genesis is usually related to a trough
or horizontal wind shear. This trough is typically observed in the lower
levels for genesis in the ITCZ region and in the upper levels for em-
bedded genesis in the trade winds.

This paper is an evaluation of typhoon genesis occurring in or near
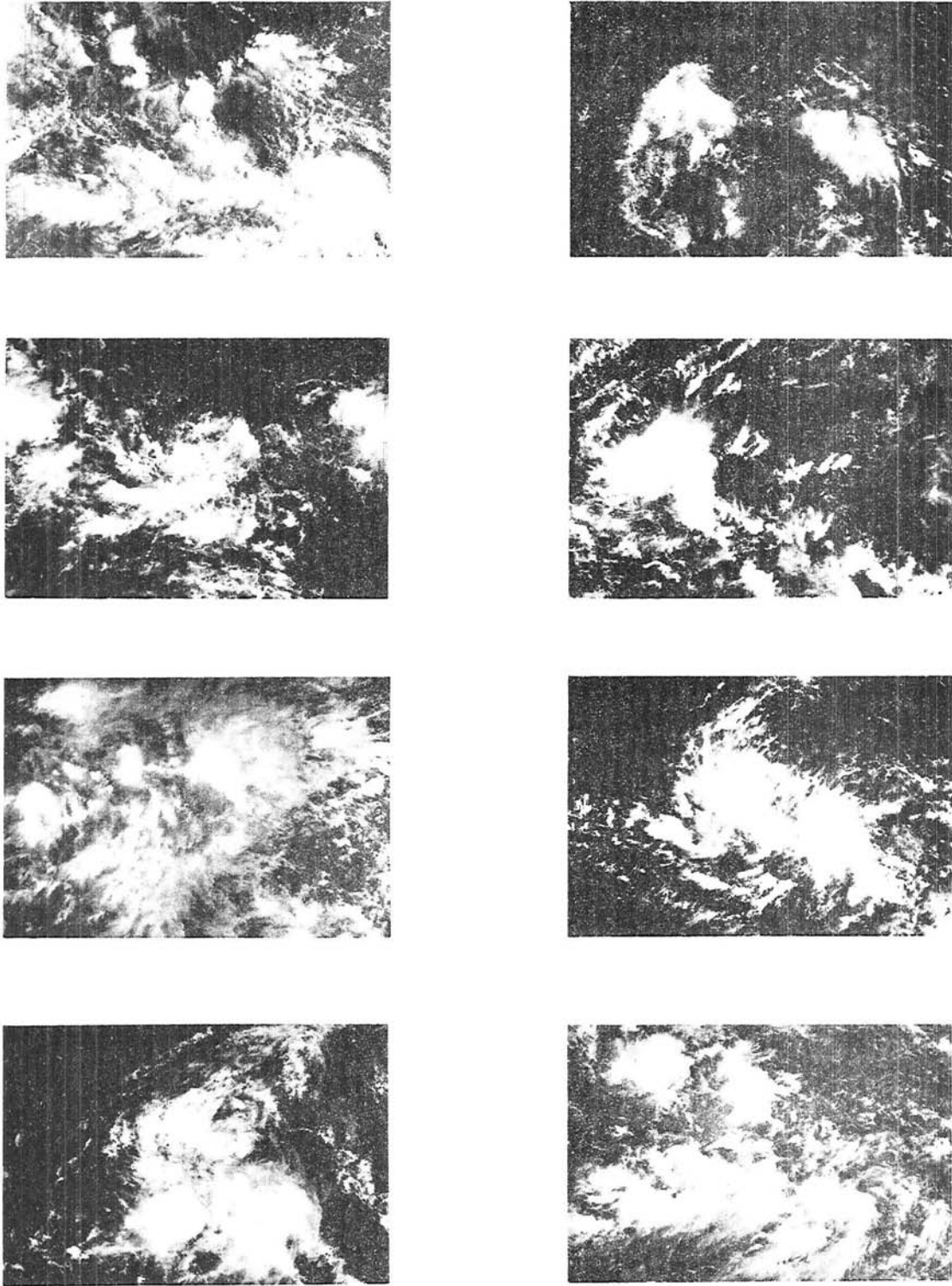the equatorial trough (Type A). Individual typhoons which appeared to

Pre-typhoon Clusters

Fig. 1. DMSP satellite pictures of pre-typhoon cloud clusters and non-developing cloud clusters. Approximate scale ⊢————⊣
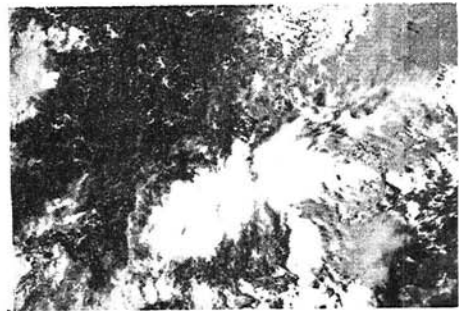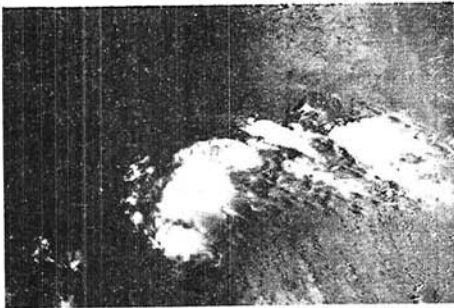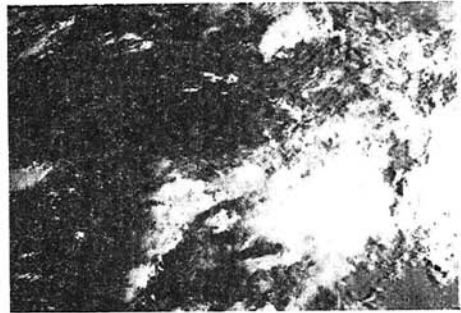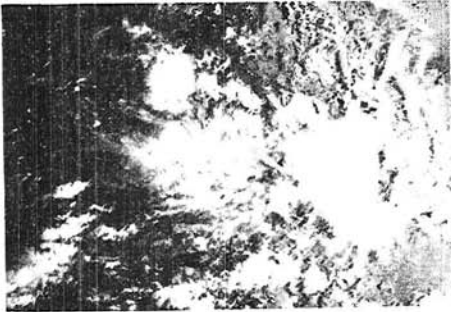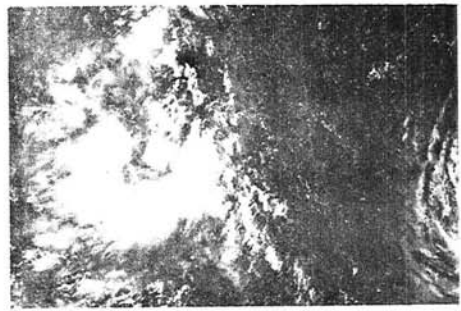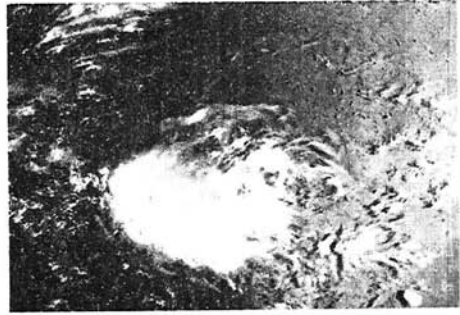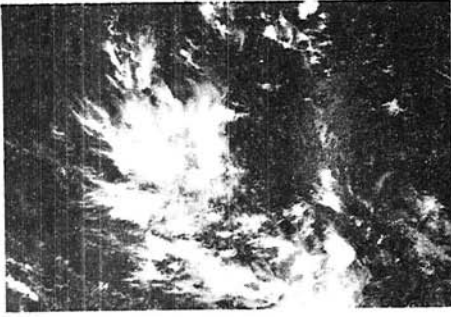500 km

Non-developing clusters

Fig. 1. Continued.

originate as a disturbance embedded in trade-wind flow (Type B genesis)
are not included. Also, disturbances which developed into tropical
storms but did not reach typhoon intensity are not included.

Previous studies of tropical cyclone formation have been based
mostly on individual case studies and/or theoretical speculation from
climatological or composited data sets (Dunn, 1940; Palmén, 1948; Riehl,
1948, 1950, 1954; Alaka, 1962; Yanai, 1961a, 1964; Colón and Nightingale,
1963; Sadler, 1967a, 1967b, 1974; Lopez, 1968; Fett, 1968; Gray, 1968,
1975; Nitta and Yanai, 1969). Recent theoretical work on the dynamic
aspects of the problem has been performed by Bates (1973), Lindzen (1974)
and Shapiro (1975).

This study investigates tropical cyclone genesis by comparing
rawinsonde data composited with respect to pre-typhoon cloud clusters
to data composites of non-developing cloud clusters. The differences
revealed between the data composites of pre-typhoon clusters and non-
developing clusters should give some indication of the distinguishing
physical processes which are important in the formation of these cyclones.

The major physical changes which take place when a weak tropical
disturbance intensifies into a typhoon or hurricane have been generally
established by previous observation and research. These are upper and
middle level tropospheric warming within the disturbance and formation
of a closed vortex throughout a deep layer of the atmosphere. Several
pre-typhoon cluster characteristics which induce or precede these major
changes are described and discussed in this paper.

2. DATA SAMPLE AND STRATIFICATIONS

2.1 Data Sources

A comparison of the basic physical features of pre-typhoon cloud clusters and non-developing cloud clusters was desired in order to investigate tropical cyclone genesis. Large numbers of rawinsonde observations were composited with respect to the locations of non-developing cloud clusters in addition to the composites with respect to clusters which intensified and became typhoons. Rawinsonde data were available from the stations in Fig. 2 at 00Z (08-12 local time) and 12Z (20-00 local time) for all data sets. The data were derived from four main sources:

1) Pre-typhoon disturbances from the time these were first identifiable as cloud clusters to when they attained an intensity with maximum sustained surface winds of 50 knots. The disturbances were located in the central and western North Pacific during the ten-year period of 1961-1970. Storms originating west of 125°E longitude (i.e., the South China Sea) were not included. Several stratifications of data, representing increasing stages of development were obtained from this data source.

2) Non-developing cloud clusters with positions originally documented by Williams and Gray (1973) and Ruprecht and Gray (1976). Clusters in the central and western Pacific during the period 1967-1968, were included. These were within the region from the equator to 18°N and from 125°E to 160°W. This data set is referred to as Stage 0.

3) Non-developing cloud clusters limited to locations in the western Pacific and to the months of June through September during 1967 and 1968. These were within the region from the equator to 18°N and from 125°E to 165°E. This data set is referred to as Stage 00.

4) Tropical storm and typhoon data supplied by W. Frank (1976). This data set represents storms south of 30°N latitude in the western North Pacific during the ten-year period, 1961-1970. Stratifications by intensity were used according to the reported central sea-level pressures.

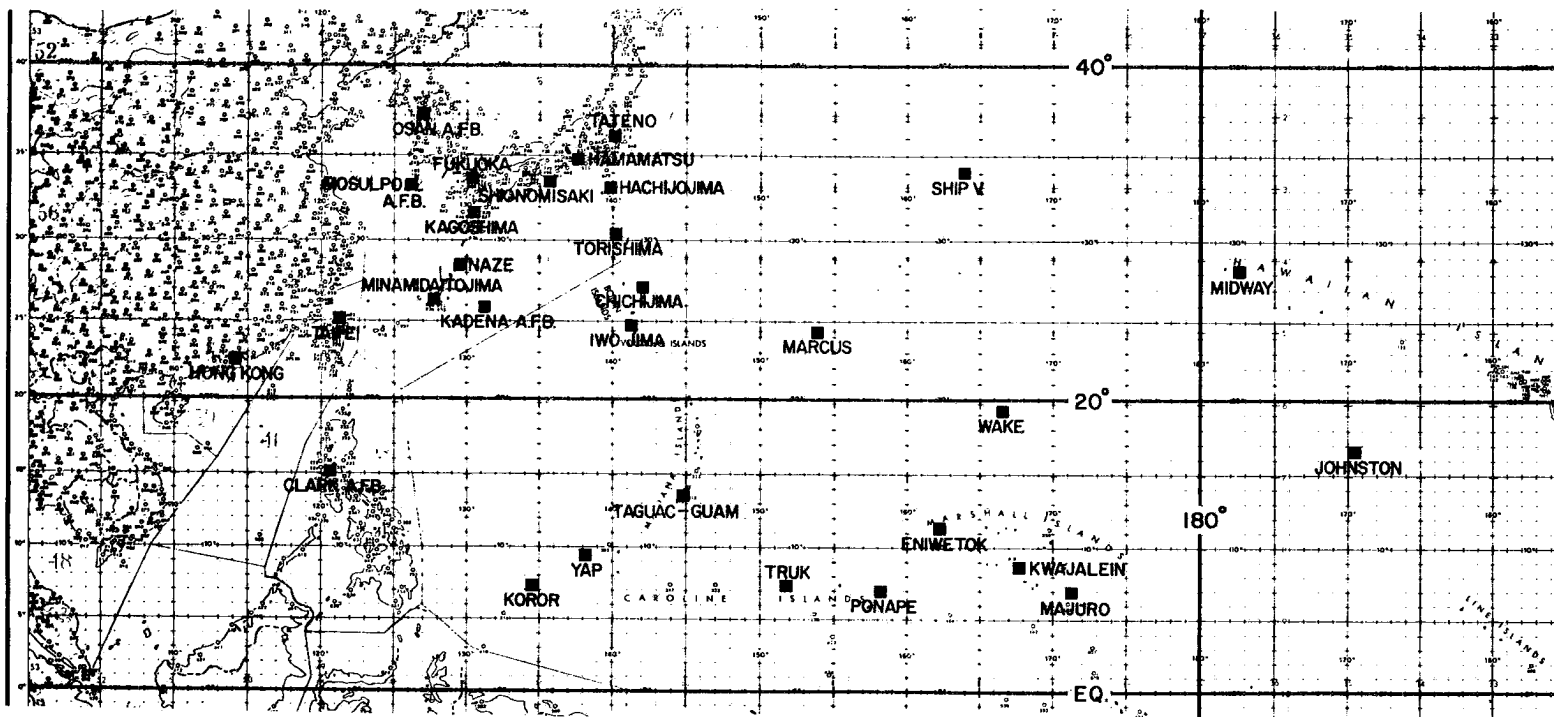These data sources allow a comparison of non-developing cloud

6

Fig. 2. Western Pacific radiosonde stations which supplied the data used in this study. Observations were taken at 00Z and 12Z which correspond to 08 LT - 12 LT and 20 LT - 00 LT respectively. Data from many of the Japanese stations north of 25°N were not applicable to this study.

clusters and pre-typhoon cloud clusters. In addition, the pre-typhoon data can be combined with the tropical storm and typhoon data of W. Frank (1976). A complete step-by-step picture of the genesis and intensification process over a wide range of intensities is thus obtained.

2.2 Compositing Philosophy

With a sparse data network such as shown in Fig. 2, it is obvious that at a given time period a reliable and accurate synoptic-scale analysis of meteorological data is not possible. However, if positions of many weather systems at numerous time periods are recorded, observations can be located according to their distance and direction from the center of the appropriate weather systems. This results in a network of very dense data, which when averaged according to an appropriate grid, allows an analysis of the mean fields of meteorological parameters with respect to the system.

This procedure undoubtedly has a significant smoothing effect, especially with respect to pressure gradients, temperature gradients, and wind fields of individual cases. The variability of the weather system and uncertainty in positioning of individual systems determines the extent to which features are smoothed out. Nevertheless, if the characteristics of the individual cases are basically similar, then the relevant physical processes should be portrayed. The success of previous rawinsonde compositing studies (Williams and Gray, 1973; Ruprecht and Gray, 1976; George and Gray, 1976, 1977 and W. Frank 1976) lends much confidence to this research methodology.

In tropical regions, meso-scale and cumulus scale processes are relatively important and often locally dominate over the influences

of the relatively weak synoptic-scale disturbances. Therefore, a single rawinsonde observation may not be representative of synoptic-scale features. Averaging large quantities of data will tend to obliterate the meso-scale features, while the synoptic-scale features will persist. However, many characteristics of the meso-scale features, such as horizontal eddy fluxes, can be preserved by proper handling of the data.

The compositing technique is especially valuable when large data samples are available. These can be broken down or stratified according to intensity, location, or other characteristics. Comparisons will reveal basic similarities and differences. The studies by George and Gray (op. cit.) and W. Frank (op. cit.) have well verified the utility of this compositing approach for tropical cyclones in the western Pacific.

2.3 Compositing Procedure

Observations were composited according to their positions relative to the centers of tropical disturbances or cloud clusters. Rawinsonde data was positioned on the circular grid shown in Fig. 3. The grid was centered on the disturbance and oriented with Octant 1 toward the north. Whenever available rawinsonde soundings fell on the grid at a given time period for a given storm, each sounding was located relative to the storm center in cylindrical coordinates. All of the parameters to be composited, whether directly measured or computed from the directly measured parameters, were determined at the observation station locations at 19 vertical pressure levels. After all parameters were either measured or computed for each sounding, the value of each parameter was assigned to a point at the center of the grid space in which the sounding fell. All soundings which fell in that grid space for the particular group of storms and time periods being analyzed were averaged.
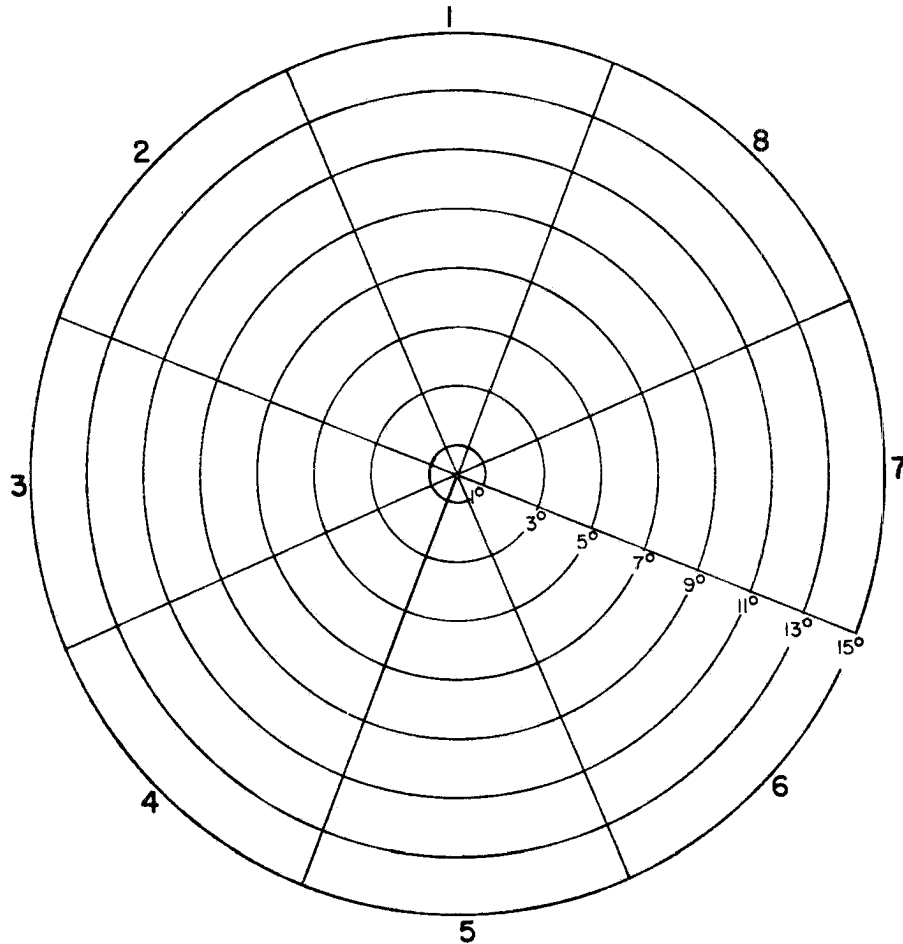
Fig. 3. Grid used to composite rawinsonde data. The grid consists of eight octants and eight radial bands, so that observations were averaged in each grid area resulting in an 8 x 8 array of values. The grid was centered on the disturbance. Octant 1 was oriented to the north (1 degree latitude/longitude = 111 km).

Data was composited at the surface and at the following pressure levels (in millibars): 1000, 950, 900, 850, 800, 700, 600, 500, 400, 300, 250, 200, 150, 100, 80, 70, 60, and 50. The parameters composited in each separate data stratification are listed in Table 1.

Computations were made in both stationary and moving coordinate systems. In the stationary system the actual observed winds were composited. In the moving system the observed propagation vector of each disturbance was subtracted from each observed wind before

TABLE 1

Parameters Averaged on the Composited Rawinsonde Data

__WINDS__

u	=	East-west component of wind
v	=	North-south component of wind
V_R	=	Radial wind
V_T	=	Tangential wind
DIV	=	Divergence
ζ	=	Relative vorticity
u_m	=	East-west component (moving coordinate system)
V_{rm}	=	Radial wind (moving coordinate system)

__THERMODYNAMIC__

Z	=	Geopotential height of standard pressure levels (actual surface pressures are composited at the surface)
T	=	Temperature
RH	=	Relative humidity
q	=	Water vapor mixing ratio
T_v	=	Virtual temperature
θ	=	Potential temperature
θ_v	=	Virtual potential temperature
θ_e	=	Equivalent potential temperature
θ_{es}	=	Saturated equivalent potential temperature

averaging. The resulting winds are the observed winds relative to the moving disturbance.

For all disturbances included in the sample, it was necessary to determine positions according to latitude and longitude at the observation times of 00Z and 12Z. This was done with the aid of satellite pictures when available and the individual storm analyses of the Joint Typhoon Warning Center (JTWC) as published in the Annual Typhoon Reports (1961-1970). The direction and propagation speed of the disturbance at each observation time was also determined.

The major source of error in this procedure was the uncertainty in positioning the disturbances. When compositing data around systems with tropical storm and typhoon intensities, this problem is minimal because of the frequent positioning by aircraft reconnaissance. With the non-developing cloud cluster data sources, all positioning was done with the aid of satellite pictures. Extrapolations were made from the daily satellite picture times to approximate time varying cluster positions. No information about the sea-level pressure or low-level wind patterns was available to aid in positioning, as was the case with the tropical storm and typhoon data.

The positions of disturbances which eventually became typhoons were determined with the aid of aircraft reconnaissance and satellite pictures. However, daily satellite pictures were not available during the 1961-1965 period, and the first position established by aircraft was often at the stage of an intensifying tropical depression. In these cases, positions were extrapolated backward in time for a day or two to establish the approximate location of the weaker cloud cluster. The analyses in the Annual Typhoon Reports were often helpful in this regard.

Undoubtedly some positioning errors are present and degrade to
some degree the quality of the composited data. However, the errors are
probably random in distribution and the effects minimal except at small
distances from the data composite center. It is believed that the un-
certainty in positioning did not prevent the consistent large-scale
features from being well portrayed.

As an example of the distribution of rawinsonde observations with
respect to the disturbance, Fig. 4 has been constructed. This figure
shows the number of observations located and averaged within each grid
area. This example is for the "Pre-typhoon" data set (explained in
Section 2.5).

In general, there are only about four observations within the entire
15° radius grid for each time period. This clearly indicates that a
quantitative analysis of these systems using conventional rawinsonde
data must employ a compositing procedure.

2.4 Balloon and Cluster Position Corrections

Corrections in the relative positions of the balloon and cluster
center are made. The relative positions of the cluster and the balloon
change due to the motions of both during the balloon's ascent time were
estimated and appropriate corrections are made.

A constant balloon ascent rate of 5 m/sec is assumed, and the
ascent time to each pressure level is estimated. A cluster speed vector
is estimated for each cluster time period from the mean cluster direction
and velocity reported ±6 hours from balloon release time. The cluster's
position is moved backward along its motion vector a distance equal to
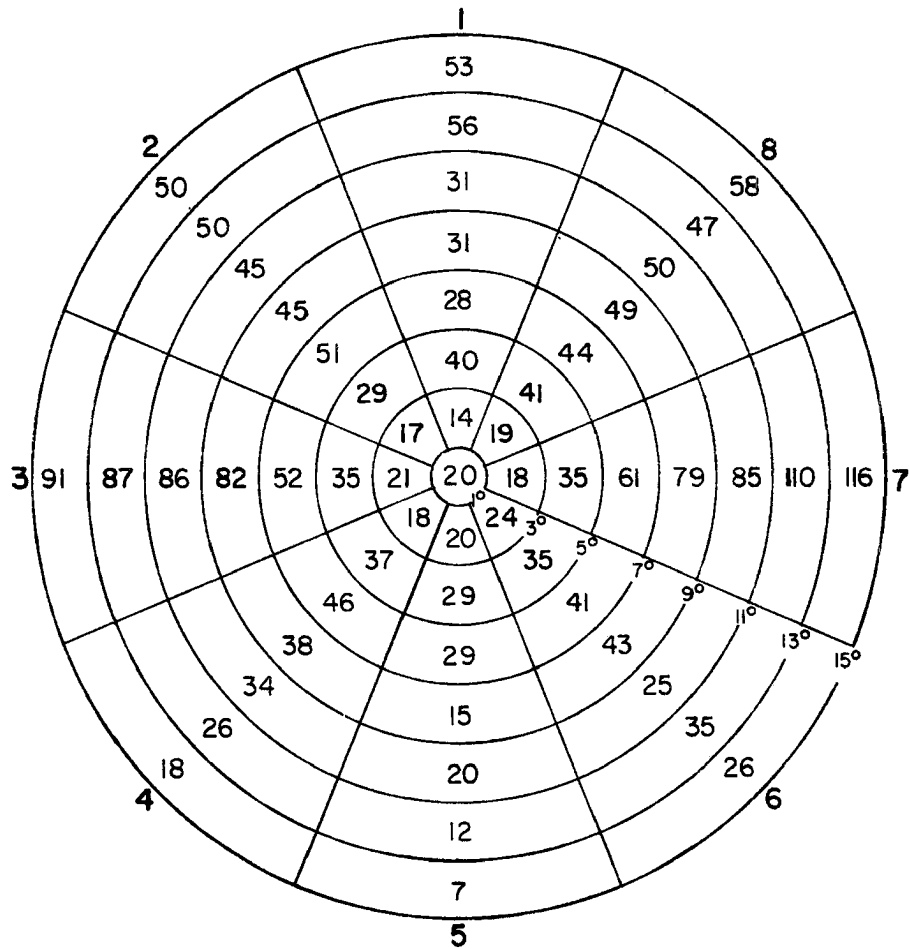30 minutes travel to account for early balloon release time. This is

Fig. 4. Number of rawinsonde observations included in the grid areas
for a particular data set. This example is for the "Pre-
typhoon" data (explained in Section 2.5).

the estimated cluster position for the surface observations. The cluster

is then moved along its cluster motion vector according to the assumed

ascent time to each level.

The balloon position is adjusted by using the mean ascent times

and the observed winds at each level. As the balloon moves through a

layer, the mean u and v wind components are estimated. The products

of these winds and the ascent time give the balloon position correction

for each level.

2.5 Stratification of Data With Respect to Disturbances Which Developed into Typhoons

For each pre-typhoon disturbance, time periods were included from when the pre-typhoon cloud cluster was first identifiable until sustained surface winds attained 50 knots. Typically, this time period was about five days. The major objective in stratifying the data was to obtain a data set representing the pre-typhoon cloud cluster which excluded all time periods when well-defined intensification was occurring. This "Pre-typhoon" data set could then be compared with the non-developing cluster data sets to determine differences.

The first aircraft observations of central sea-level pressure and maximum sustained winds for a particular pre-typhoon disturbance usually indicate about 1000 mb and 30 knots respectively. The data were stratified into two groups by going back one day (two time periods) before this first aircraft observation. All time periods before this "first observation minus one day" point, were included in a data set named "Pre-typhoon". All time periods after this point were included in a data set named "Intensifying". In a few cases, when the first aircraft observation indicated a more intense system, the stratification would be made by going back 1½ or 2 days. This stratification essentially divided the data into two approximately equal parts. The first half ("Pre-typhoon") represents a pre-typhoon cloud cluster with appearance similar to the non-developing cloud clusters and little or no evidence of tropical cyclone characteristics. The second half ("Intensifying") represents an intensifying tropical depression. The disturbance is very weak at this latter stage, although it is organized and intensifying.

The possibility that the later pre-typhoon time periods might include some intensifying disturbances was considered. Thus, a data set was assembled which included only the first day and a half of the pre-typhoon cluster's recognized existence. This data set was named "Initial".

An additional data set arbitrarily named "Genesis" represents the transition period from "Pre-typhoon" to "Intensifying". Data from the last day of the "Pre-typhoon" period and the first day of the "Intensifying" period comprised this data set.

As a result of these stratifications, the entire data set was subdivided into four progressive stages in time. These were numbered: Stage 1, "Initial"; Stage 2, "Pre-typhoon"; Stage 3, "Genesis"; Stage 4, "Intensifying". These stages overlap in time and are depicted in Fig. 5 for a typical case. Also shown in Fig. 5 are Stages 5 and 6. These were data sets supplied by W. Frank (1976) and were stratified according to observed central sea-level pressure. These were easily integrated to depict six stages of development with Stage 5 representing central pressures of 980-1000 mb and Stage 6, 950-980mb. In general, Stage 5 is indicative of "tropical storm" intensity, and Stage 6 represents "typhoon" intensity.

The two data sets representing the non-developing cloud clusters have been described in Section 2.1. The general data set originating from the Ruprecht and Gray (1976) study is Stage 0. The restricted data set, representing only summer season clusters in the western Pacific, is Stage 00. These are used as a basis of comparison with the pre-typhoon cluster data sets represented by Stages 1 and 2.

Table 2 summarizes the average geographical location and movement of the disturbances in each data set. Table 3 lists the sea-level
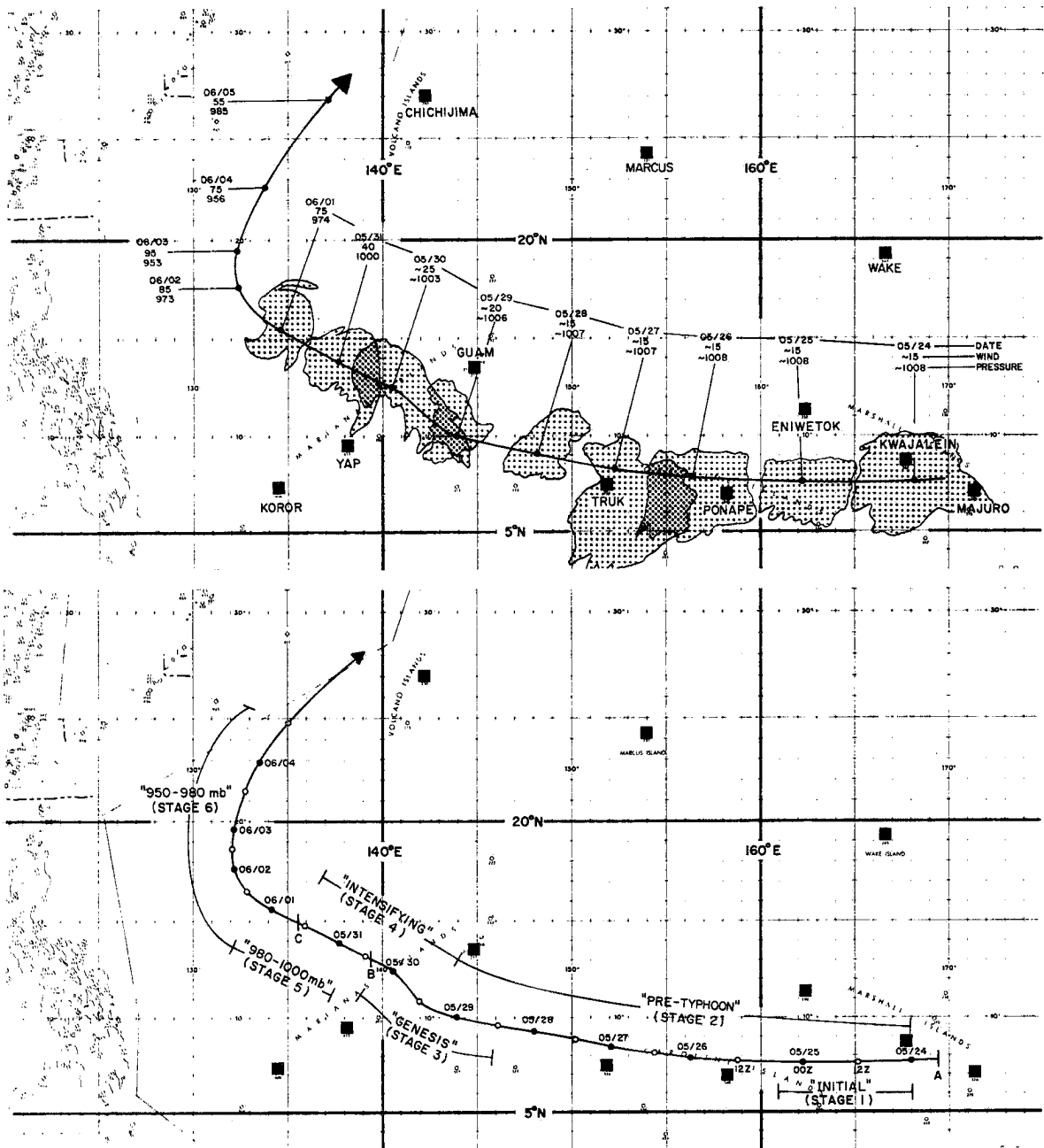
Fig. 5. Typical example depicting the various stages of development during pre-typhoon and mature stages. This storm is Typhoon Kim occurring 31 May - 05 June, 1968. The radiosonde stations are indicated by solid squares. The top figure shows the cloud cluster shape of the disturbance as indicated by satellite pictures. The maximum sustained surface winds (knots) and minimum sea-level pressures (mb) are given. The bottom figure shows the various stages defined in this study. Point A represents the time when the pre-typhoon cluster was first identifiable. Point B represents the first observation by aircraft reconnaissance. Point C is where the disturbance attained sustained surface winds of 50 knots.

pressures and surface winds associated with the various data sets. The sizes of the data samples and the approximate time periods represented by the particular stages are given in Table 4.

TABLE 2

Mean Characteristics of Data Sets

Data Set	Latitude (^{O}N)	Longitude	Direction (from which disturbance is moving) (degrees)	Speed of Movement (m sec^{-1})
Non-developing (Stage 0)	10.6	158.9	90.0	7.5
Non-developing (Stage 00)	10.9	148.7	94.1	7.4
"Initial" (1)	9.3	154.9	98.3	5.7
"Pre-typhoon" (2)	10.2	152.5	107.3	5.5
"Genesis" (3)	11.7	147.7	111.5	5.5
"Intensifying" (4)	13.5	143.6	117.6	5.1
*"Tropical storm" (980-1000 mb) (5)	19.3	136.3	139.3	4.9
*"Typhoon" (950-980mb) (6)	21.5	136.0	146.3	5.0

19

* Data from W. Frank (1976), all tropical storms or typhoons south of 30°N with observed central sea-level pressures between the noted limits.

TABLE 3

Mean Surface Pressures and Winds

Data Set	Estimate of Central Sea-level Pressure (mb)	Measured Mean Sea-level Pressure(mb)Within 3° Latitude of Disturbance Center	Estimate of Maximum Sustained Surface Winds (knots)	Measured Mean Surface Wind (knots) Within 3° Latitude of Disturbance Center
0	1008	1010.3	15	9.6
00	1008	1010.1	15	7.0
1	1007	1010.0	15	7.4
2	1005	1009.0	15	7.5
3	1003	1008.0	20	9.0
4	1000	1007.1	35	11.5
5	990	1005.0	50	14.3
6	965	1003.5	80	21.0

TABLE 4

Sample Sizes and Representative Time Periods of the Data Sets

Data	Stage No.	Total Number of Observations	Number of Individual Disturbances	Approximate Time Period Represented
Non-developing	0	10197	~400	2-3 days(entire lifetime of cluster)
Non-developing	00	1991	87	2-3 days(entire lifetime of cluster)
"Initial"	1	943	130	first day of pre-typhoon cluster
"Pre-typhoon"	2	2404	130	2-3 days (pre-typhoon cluster)
"Genesis"	3	2040	130	2 days (formative stages of a tropical depression)
"Intensifying"	4	2672	130	2-3 days (intensifying tropical depression)
"Tropical Storm"	5	5658	~200	2 days (tropical storm intensity)
"Typhoon"	6	4573	~175	2-5 days (typhoon intensity)

3. COMPARISON: NON-DEVELOPING CLUSTER AND PRE-TYPHOON CLUSTER

In general, typhoons develop from cloud clusters which are similar in satellite observed appearance to non-developing cloud clusters. A more-detailed comparison of the pre-typhoon clusters and the non-developing clusters from DMSP satellite data will be discussed in a forthcoming report by Erickson (1977). In this study the rawinsonde composites representing the pre-typhoon cloud cluster, Stages 1 and 2, are extensively compared with two non-developing cloud cluster data sets, so named Stages 0 and 00. Including both non-developing cluster data sets allows some of the consistent features of non-developing clusters to be differentiated from more variable features. The Stage 00 data is essentially a subset of the larger more general Stage 0 data set, as depicted on the map of cluster locations in Fig. 6. Stage 00 was restricted to the months of June through September.

The rawinsonde data in the 3-5° radius band is chosen as best representative of the characteristics of the cluster's edge or perimeter. Large data samples are then available to describe the relatively small but very important features such as surrounding cluster radial wind and water vapor import. This data is applicable at 4° radius which defines a mean cluster of 8° diameter (888 km). Although this is a very large region, many ITCZ clusters do have horizontal extent on the order of 8° latitude. The rawinsonde data composited in the 0-3° radius region is chosen as best representative of the mean thermodynamic characteristics such as temperature and humidity. The number of soundings included in each of these key areas for each cluster data set is listed in Table 5.
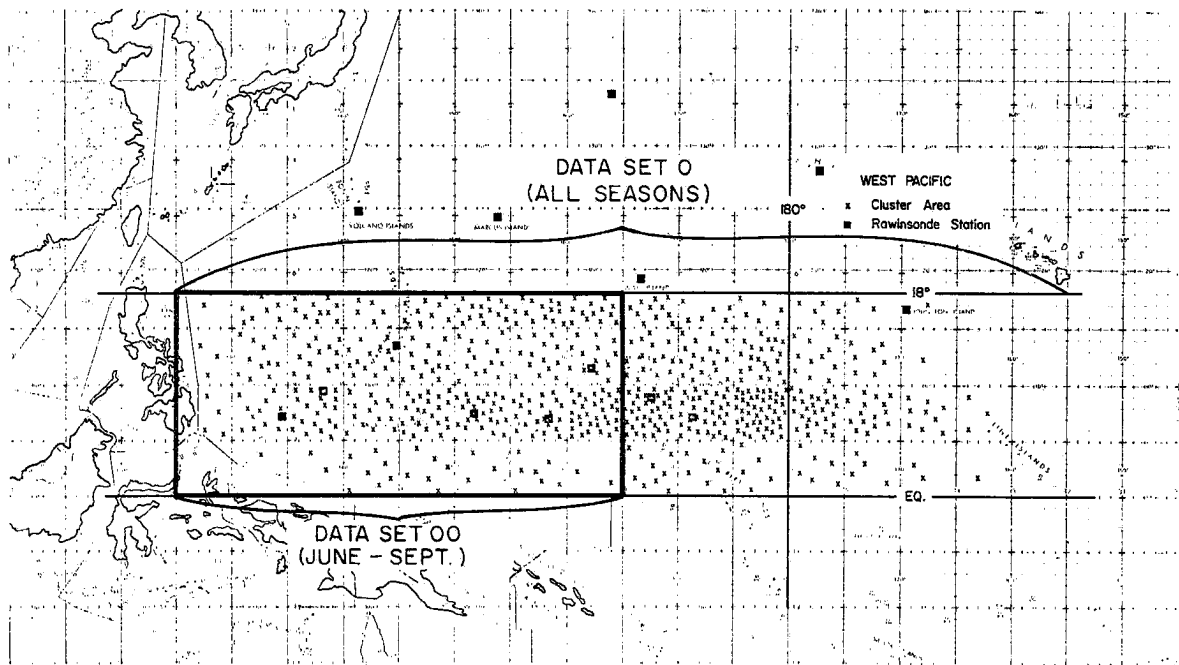
Fig. 6. X's mark positions of the clusters included in the non-developing cluster data set, Stage 0. Clusters were included which existed during all seasons. Non-developing cluster data set, Stage 00, included clusters only in the enclosed region and only during the months of June through September.

TABLE 5

Number of Rawinsonde Soundings Included in the Composites

Data Set	$r = 0\text{-}3^{o}$	$r = 3\text{-}5^{o}$
Non-developing		
00	167	224
0	781	1122
Pre-typhoon		
1	67	105
2	171	281

3.1 Surface Pressure

The 1000 millibar height patterns for the pre-typhoon (Stage 2) and non-developing clusters (Stages 0 and 00) are shown in Fig. 7. The observed height minima are equivalent to sea-level pressure minimums of 1008-1009 mb in the vicinity of the cluster. Both cluster systems have surface pressures slightly lower than the surrounding regions. The pre-typhoon clusters and non-developing clusters possess no large surface pressure pattern differences. The pressure gradient to the north of the pre-typhoon cluster is significantly larger than that of the 00 Stage however.

3.2 Mean Soundings and Lapse Rates

The mean temperature lapse rates within each disturbance are also very similar. The mean geopotential heights (Z), temperatures (T), relative humidities (RH), and water vapor mixing ratios (q), at the various levels for the non-developing and pre-typhoon clusters are listed in Table 6. The mean soundings from the Stage 00 and Stage 2 data sets for the r = 0-3$^{\text{o}}$ area are shown. The corresponding mean sounding for Stage 0 was nearly identical to Stage 00. Although differences are small at all levels, there are very significant differences in vertical temperature structure and water vapor contents. These are described in detail in Sections 3.6 and 3.7, respectively.

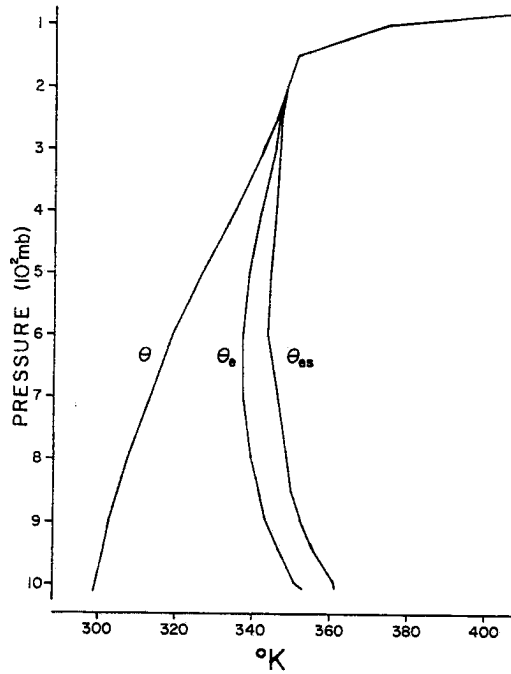The vertical profiles of potential temperature (Θ), equivalent potential temperature (Θ_e), and saturated equivalent potential temperature (Θ_{es}) are shown in Fig. 8 for the pre-typhoon cluster (Stage 2). The potential temperature increases almost linearly with decreasing pressure throughout the troposphere. The mean vertical profiles of potential temperature and saturated equivalent potential temperature are very similar within the non-developing clusters. Figure 9 depicts the vertical profiles of equivalent potential temperture within the pre-typhoon
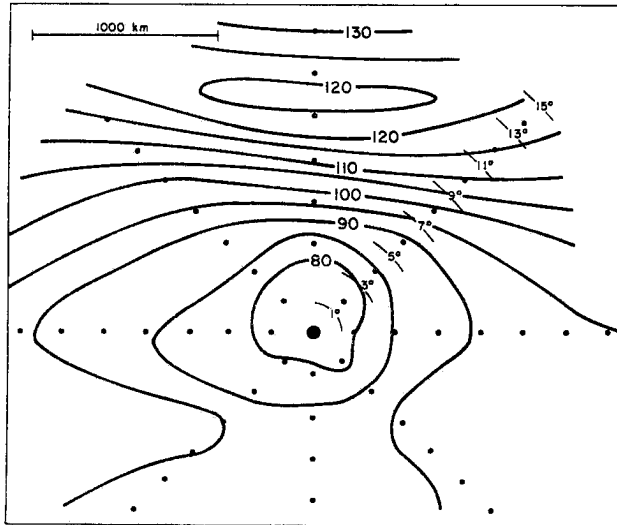
Pre-typhoon cluster
(Stage 2)
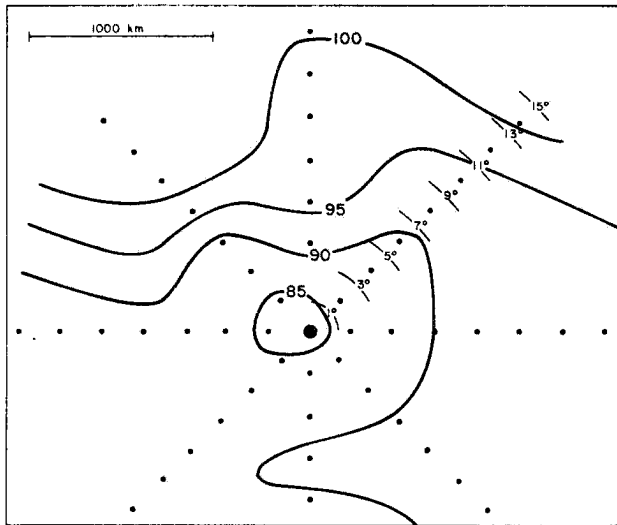
Non-developing cluster
(Stage 00)
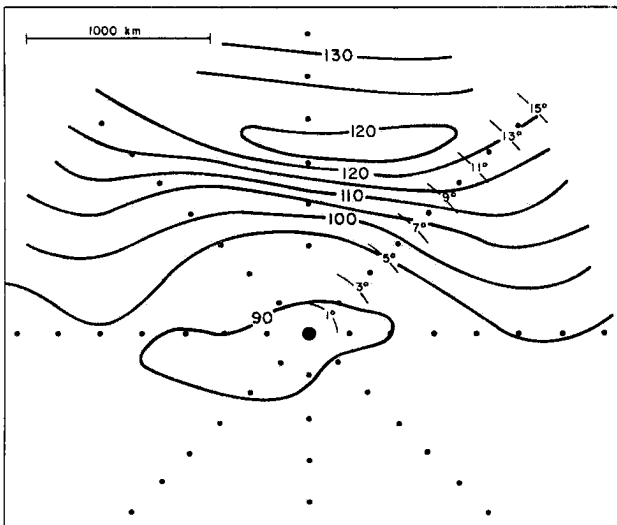
Non-developing cluster
(Stage 0)

Fig. 7. 1000- millibar geopotential heights (meters). The 5-meter
interval is equivalent to about ½ mb of pressure.

TABLE 6

Mean Soundings Within Cluster Area (r < 3°)

	Pre-Typhoon(2)				Non-Developing (00)				Differences (2) - (00)			
P(mb)	Z(meters)	T($^{\circ}$C)	RH(%)	q(gkg^{-1})	Z(meters)	T($^{\circ}$C)	RH(%)	q(gkg^{-1})	Z(meters)	T($^{\circ}$C)	RH(%)	q(gkg^{-1})
70	18662.2	-69.5			18662.2	-68.6			.0	-0.9		
80	17873.7	-73.9			17869.0	-72.4			4.7	-1.5		
100	16580.2	-78.6			16569.2	-77.3			11.0	-1.3		
150	14232.4	-68.6			14220.8	-69.0			11.6	0.4		
200	12445.0	-53.1			12438.3	-53.8			6.7	0.7		
250	10964.4	-40.4			10963.2	-40.8			1.2	0.4		
300	9693.4	-30.1	40.0	.4	9694.9	-30.4	47.9	0.5	-1.5	0.3	-7.9	-.1
400	7579.3	-15.3	52.4	1.5	7585.4	-15.6	62.7	1.8	-6.1	0.3	-10.3	-.3
500	5857.5	-5.3	70.6	3.6	5863.6	-5.5	73.0	3.7	-6.1	0.2	-2.4	-.1
600	4402.4	2.5	74.5	5.7	4409.2	2.2	75.7	5.7	-6.8	0.3	-1.2	0
700	3137.3	9.9	72.8	8.0	3144.7	9.5	71.2	7.6	-7.4	0.4	1.6	.4
800	2012.0	15.8	78.3	11.1	2023.4	15.5	76.5	10.6	-11.4	0.3	1.8	.5
850	1493.1	18.3	78.7	12.4	1504.8	18.2	79.2	12.4	-11.7	0.1	-0.5	0
900	999.9	20.6	81.4	14.1	1010.5	20.9	80.5	14.1	-10.6	-0.3	0.9	0
950	526.3	23.1	85.7	16.3	535.8	23.6	83.2	16.3	-9.5	-0.5	2.5	0
1000	75.1	26.0	87.0	18.8	86.6	26.0	86.7	18.7	-11.5	0	0.3	.1
SFC	-------	26.1	88.6	19.2	-------	26.1	88.0	19.0	-----	0	0.6	.2

Fig. 8. Potential temperature (θ), equivalent potential temperature (θ_e), and saturated equivalent potential temperature (θ_{es}) in the r = 0-3° area for the "Pre-typhoon" (Stage 2) data set. (°K).
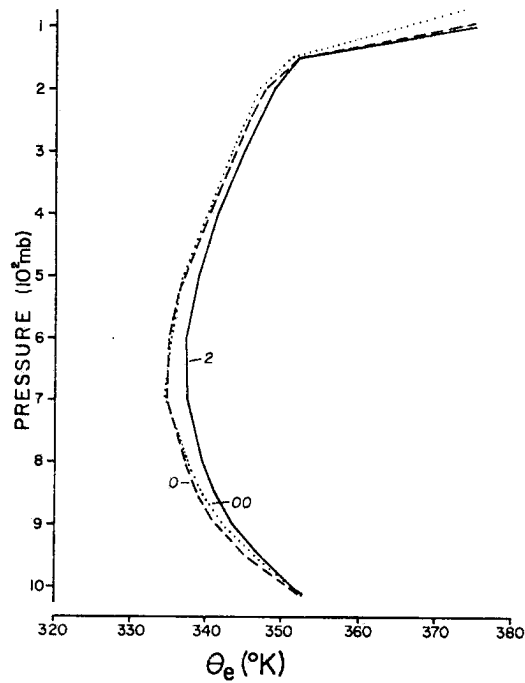
Fig. 9. Equivalent potential temperature (θ_e) (°K) in the r = 0-3° area for the non-developing cluster data sets (Stages 0 and 00) and the "Pre-typhoon" (Stage 2) data set.

(Stage 2) and non-developing (Stages 0 and 00) clusters. From Figs.
8 and 9 it is clear that the stabilities and potential buoyancies are
very similar with both systems.

3.3 Divergence and Vertical Motion

The vertical profiles of divergence for the $r = 0-4^{\circ}$ area are shown
in Fig. 10. The mean radial winds in the radial band, $r = 3-5^{\circ}$, were
assumed to represent the radial winds at $r = 4^{\circ}$. Inflow is observed
through a large depth of the atmosphere (surface to 400 mb) and outflow
is concentrated between 100 mb and 300 mb.

Figure 11 shows the corresponding mean vertical velocity (ω) profiles
for the pre-typhoon cluster (Stage 2) and non-developing clusters (Stages
0 and 00). These were derived kinematically from the radial winds at 4°
radius. ω represents the mean vertical mass flow (negative values denote
upward motion) within the 8° diameter area centered on the cluster. Local
values of vertical velocity may be considerably different than the mean
cluster area value. The profiles of mean vertical velocity (ω) indicate
somewhat larger mean upward motion in the pre-typhoon cluster than
the non-developing cluster. The maximum mean upward motion is about
25% greater with the pre-typhoon clusters. These results agree with
recent findings of Erickson (1977) in which a statistical analysis
of DMSP satellite shows more deep convection occurring at $2-4^{\circ}$ radius in
developing cloud clusters than in non-developing clusters. Mean vertical
motion is correlated to the amount of deep cumulonimbus convection.

Maximum upward values of mean vertical velocity range from about
140 to 200 mb per day in the 300 to 400 mb layer. Since these results
apply to an 8°-diameter region, they agree quite well with the cloud
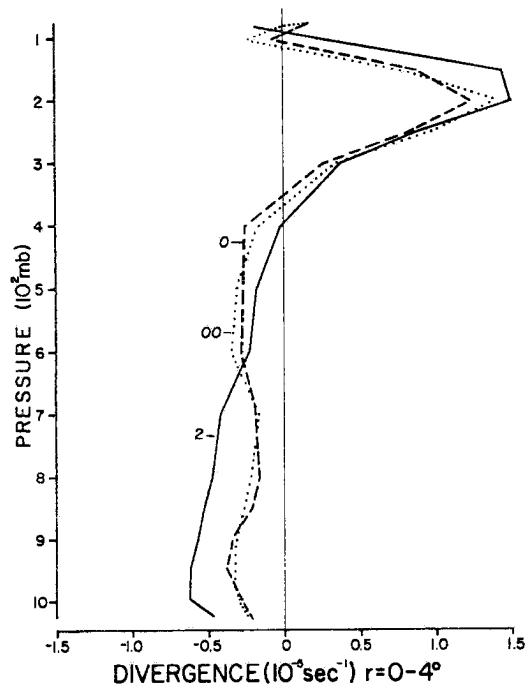
Fig. 10. Mean divergence within the r = 0-4° area for the pre-typhoon cluster (2) and the non-developing clusters (0) and (00).
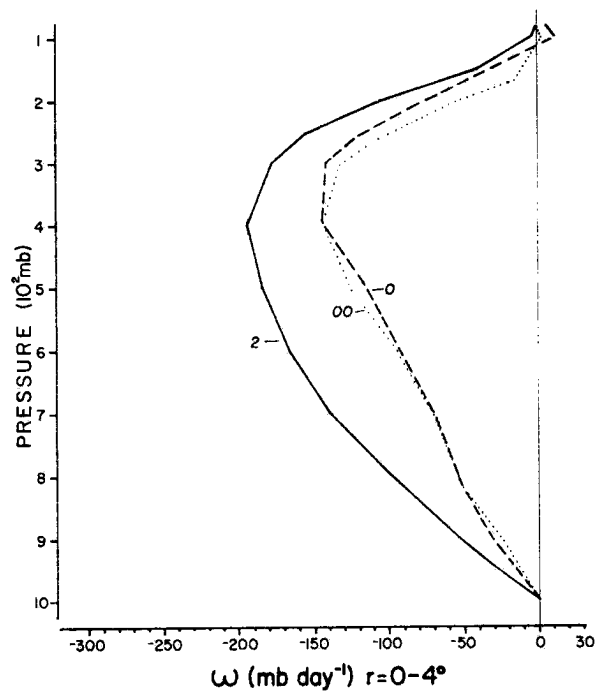
Fig. 11. Mean vertical velocity (ω) in the r = 0-4° area for the pre-typhoon cluster (2) and the non-developing clusters (0) and (00).

cluster vertical motion profiles of Williams and Gray (1973), and

Ruprecht and Gray (1976). Reed and Recker's (1971) composited rawin-

sonde data with respect to the trough region of 18 easterly waves also

indicate similar mean vertical motion patterns.

3.4 Water Vapor Budget

The import of water vapor at $r = 4^{\circ}$ integrated through the tropo-

sphere added to an assumed evaporation rate of 0.5 g cm^{-2} day^{-1} gives

an estimate of the mean rainfall rate within the cluster ($r = 0-4^{\circ}$).

This is based on the assumption that the total quantity of vapor and

liquid water remains approximately constant. Figure 12 depicts the

total vapor transports at $r = 4^{\circ}$ for the pre-typhoon and non-developing

clusters. The integrated vapor imports in g cm^{-2} day^{-1} are also given.

These total transports were computed by compositing $V_R q$ products (where

V_R is the radial wind and q is specific humidity) for the individual

soundings. The total transport $\overline{V_R q}$ consists of a mean $(\overline{V_R}\ \overline{q})$ and eddy

$(\overline{V_R' q'})$ term. Using a typical evaporation rate of 0.5 g cm^{-2} day^{-1},

mean cluster rainfalls of about 2.0-2.5 g cm^{-2} day^{-1} (cm day^{-1}) are

indicated. These results are similar to those obtained by Williams and

Gray (1973).

The impression of some previous researchers has been that heavily rain-

ing systems often do not develop into typhoons and that the intensity

of cumulus convection is not well related to tropical cyclone genesis.

The present observations that the mean vertical motion, lapse rates,

and water vapor imports are not greatly different with non-developing

and pre-typhoon cloud clusters support this impression. The mean

rainfalls associated with each cluster system are apparently not greatly
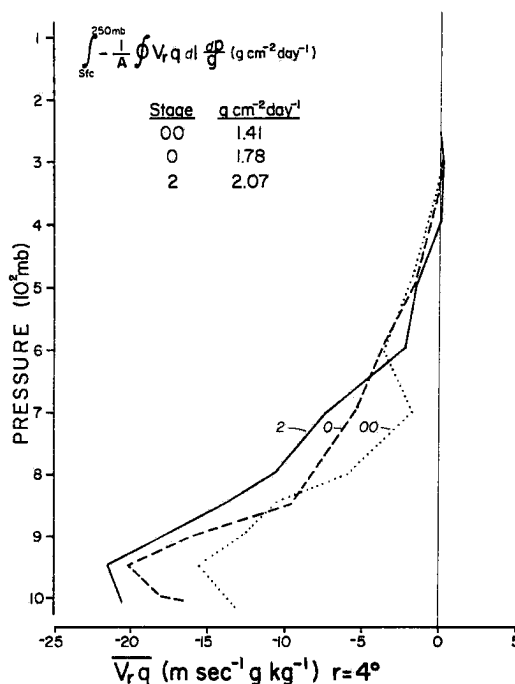
Fig. 12. Total water vapor divergence $\overline{(V_R\ q)}$ at $r = 4°$ for pre-typhoon cluster (2) and non-developing clusters (0) and (00). The vertically integrated transports are also shown in g cm^{-2} day^{-1}.

different, although the developing cluster, on the average, has about 20% more rainfall.

3.5 Low-Level Vorticity and Wind Patterns

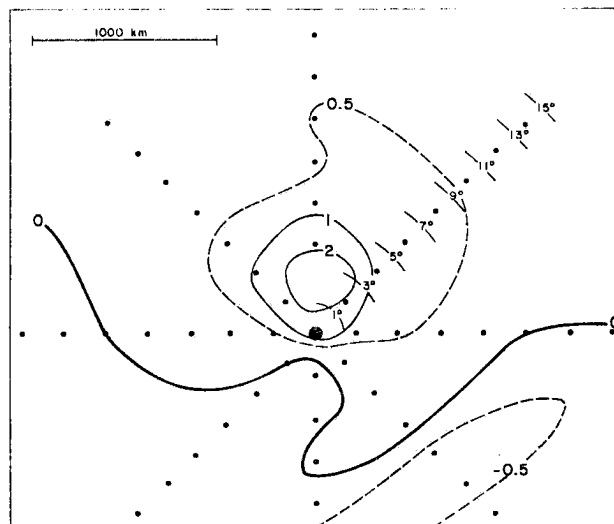The 900-millibar relative vorticity fields of the mean pre-typhoon cluster and non-developing clusters are shown in Fig. 13. Note that the area with values greater than 2×10^{-5} sec^{-1} is significantly larger with the pre-typhoon cluster. In the immediate vicinity of the cluster the relative vorticity is more than twice as large in the pre-typhoon cluster as in the Stage 00 non-developing cluster. This is the most substantial difference between non-developing and pre-typhoon cloud clusters.
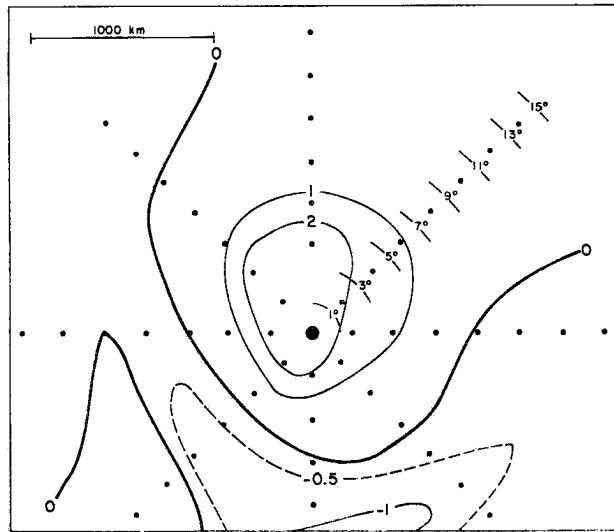
Pre-typhoon cluster
(Stage 2)
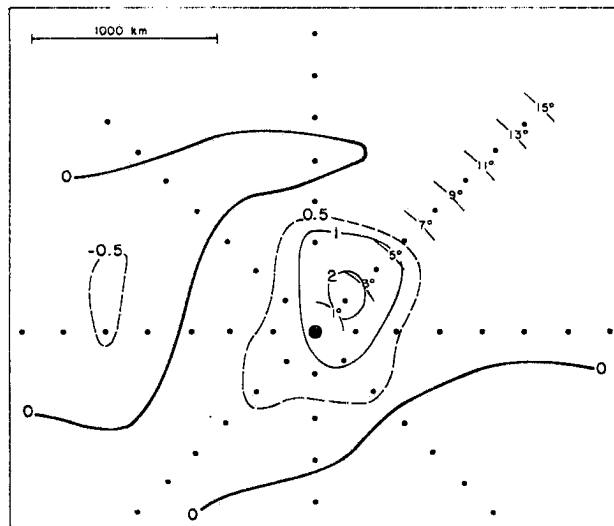
Non-developing cluster
(Stage 00)

Non-developing cluster
(Stage 0)

Fig. 13. 900-millibar relative vorticity (units are $10^{-5}\sec^{-1}$).

The isotach and streamline analyses of the low-level flow are shown in Fig. 14. The Stage 00 non-developing cluster and the pre-typhoon cluster have mean southwesterly flow to the south of their center. This type of flow pattern with respect to the Intertropical Convergence Zone (ITCZ) is referred to as the monsoon (or doldrum) trough. Many non-developing clusters which are embedded in a sheared trade wind flow typical of winter and spring conditions are included in the Stage 0 data set. This acted to average out the westerly flow to the south of a number of these clusters. The statistical average of numerous low-level flow patterns associated with non-developing clusters is depicted by Stage 0 in Fig. 14. Strong easterlies appear to the north of the cluster and weak easterlies to the south. An ITCZ with easterly flow both to the north and south is referred to as a trade wind equatorial trough. It has been recognized previously by Sadler (1967a) and Gray (1968) that the monsoon (or doldrum) trough is typically a more favorable environment for the development of tropical storms. However, as indicated by the Stage 00 cluster data set, numerous non-developing clusters exist in the doldrum trough region. Cluster existence within the trough does not guarantee intensification.

It appears that the magnitude of the low-level relative vorticity is an important factor in typhoon genesis. Table 7 lists the mean relative vorticities (ζ) within 4° radius for the various data sets representing the pre-typhoon and non-developing clusters at 900 millibars and at 600 millibars. The relative vorticities are computed from the composited mean winds, by two methods:
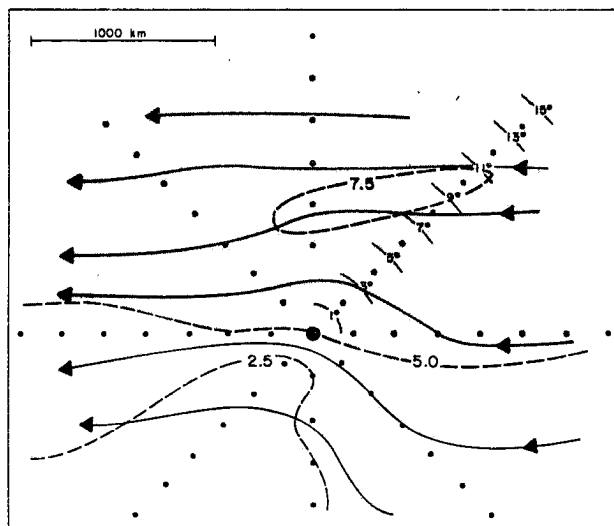
$$\bar{\zeta} = \frac{\partial v}{\partial x} - \frac{\partial u}{\partial y} \quad , \text{ and}$$
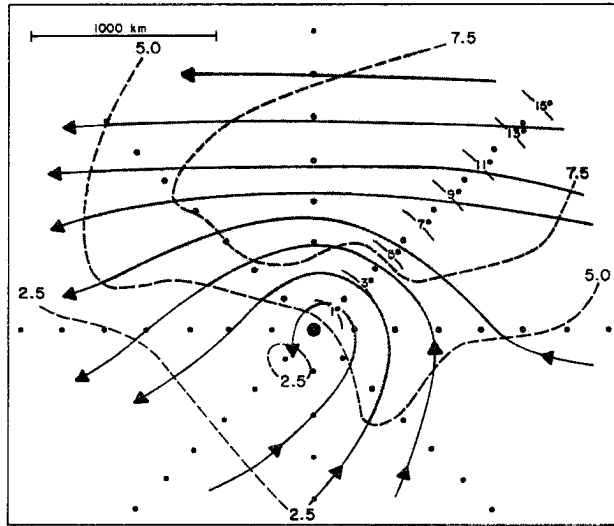
Pre-typhoon cluster
(Stage 2)
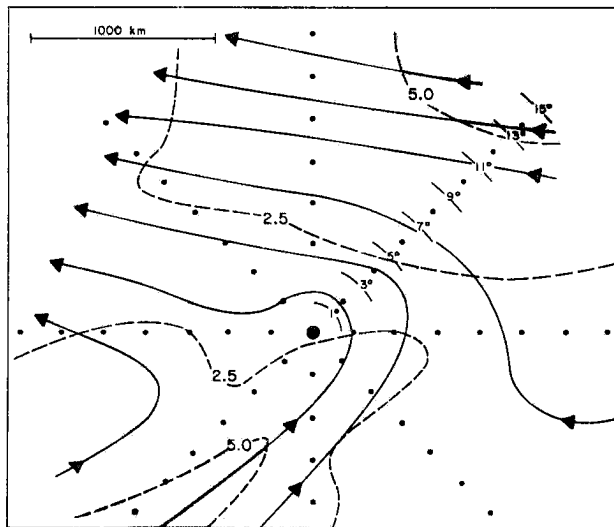
Non-developing cluster
(Stage 00)

Non-developing cluster
(Stage 0)

Fig. 14   950-millibar isotach (m sec^{-1}) and streamline analysis.

$$\bar{\zeta} \approx \frac{2\bar{V}_T}{r} \quad .$$

where $\bar{V}_T$ is the mean tangential wind around the 4° radius (r)

cluster. The contributions to the relative vorticity of the north-

south horizontal shear ($-\frac{\partial u}{\partial y}$) and the east-west shear ($\frac{\partial v}{\partial x}$) are also

given. These shears are measured across a distance of 8° latitude

(888 km) centered on the disturbance. With both cluster types the

north-south shear dominates. The east-west shear contributes a larger

proportion of the relative vorticity with pre-typhoon clusters. This

is indicative of a stronger meridional flow and/or easterly wave pattern.

These features suggest a significant difference in the low-level cyclonic

circulation of the two cluster systems.

TABLE 7

Comparison of Mean Relative Vorticity Inside 4° Radius for the Pre-
Typhoon and the Non-developing Cloud Clusters

Data Set	900 mb (10^{-5}sec^{-1})				600 mb (10^{-5}sec^{-1})			
	$\frac{\partial v}{\partial x}$	$\left(-\frac{\partial u}{\partial y}\right)$	$\left(\frac{\partial v}{\partial x}-\frac{\partial u}{\partial y}\right)$	$\frac{2\bar{V}_T}{r}$	$\frac{\partial v}{\partial x}$	$\left(-\frac{\partial u}{\partial y}\right)$	$\left(\frac{\partial v}{\partial x}-\frac{\partial u}{\partial y}\right)$	$\frac{2\bar{V}_T}{r}$
Non-Developing								
0	0.25	0.63	0.88	0.93	0.28	0.60	0.88	0.92
00	0.26	0.63	0.89	0.73	0.10	0.57	0.67	0.89
Pre-Typhoon								
1	0.68	1.07	1.75	1.81	0.61	0.39	1.00	1.22
2	0.75	1.31	2.06	2.36	0.73	0.87	1.60	1.80

The data composites of the pre-typhoon cluster suggest a more closed vortex circulation in the lower troposphere, while the non-developing cluster is characterized by a more cyclonically sheared circulation. A "closed vortex" is defined to exist at any level where the composited data indicates a positive mean tangential wind in all eight sectors around a radial band. With this definition, the "Pre-typhoon"(Stage 2) data set indicates a "closed vortex" at all levels below and including 500 mb. A "closed vortex" does not exist at any level through the atmosphere with the non-developing cluster data sets (0 and 00). This is true out to 4° radius from the cluster center.

Vertical profiles of the mean tangential wind in the $r = 1-3^O$ and $r = 3-5^O$ radial bands are depicted in Figs. 15 and 16 respectively. Assuming that these represent the tangential wind at $r = 2^O$ and 4°, $\zeta = \frac{2\overline{V_T}}{r}$ represents the mean relative vorticity within a radius r of the cluster center. Table 7 and Figs. 15-16 indicate that the relative vorticity of the pre-typhoon cluster compared to the non-developing cluster is more than twice as large in the lower troposphere. However, at middle and upper levels the differences are much smaller. The non-developing clusters have maximum positive relative vorticity in the middle troposphere.

3.6 Vertical Temperature Structure

The vertical profiles of tangential wind in Figs. 15-16 imply that the non-developing clusters (Stages 0 and 00) are cold-core systems below 600 millibars since the tangential winds are maximum at this level. In contrast, the pre-typhoon clusters (Stages 1 and 2) have maximum tangential winds in the lower troposphere, suggesting a warm-core from 900 mb to 150 mb. Vertical profiles of T_c-T_e where T_c is
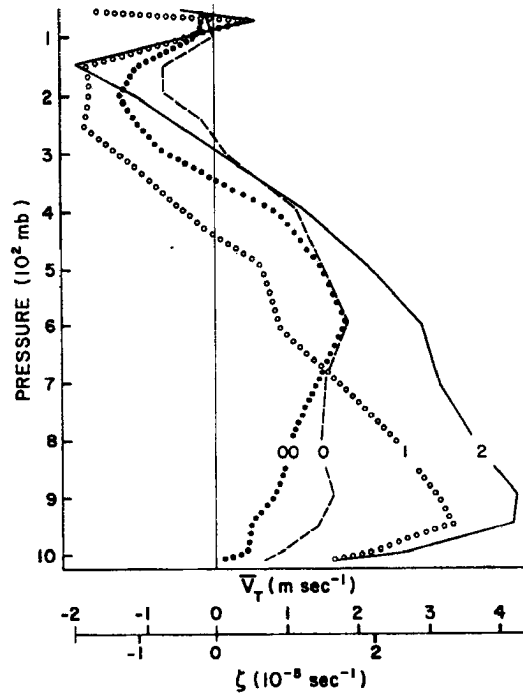
Fig. 15.   Vertical tangential wind profiles of pre-typhoon clusters (1 and 2) and non-developing clusters (0 and 00). The tangential winds shown are the mean in the r = 1-3° band, and can be interpreted as a mean relative vorticity within r = 2°.
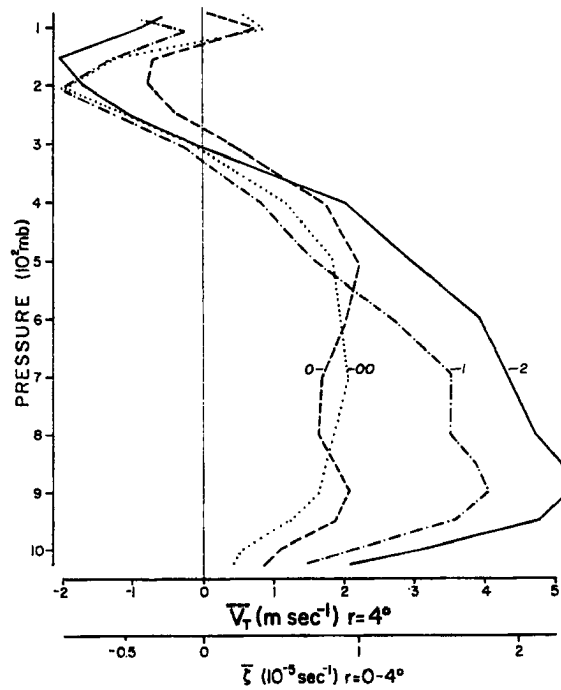

Fig. 16.   Vertical tangential wind profiles of the pre-typhoon clusters (1 and 2), and non-developing clusters (0 and 00). The mean tangential winds shown are the mean in the r = 3-5° band, and can be interpreted as a mean relative vorticity within r = 4°.

the mean temperature within the cluster region and T_e is the mean

temperature of the "environment", or surrounding region are plotted

in Figs. 17-21. The temperature gradients between the clusters and its

surroundings as revealed by the composited data are very small. The

precise configuration of the temperature structure varies somewhat depend-

ing on the area of the data composite chosen to represent the cluster

and its "environment". Five different depictions of the vertical pro-

files of T_c-T_e are shown. [Fig. 17, T_c (r = 0-1°), T_e (r = 5-7°); Fig.

18, T_c (r = 0-1°), T_e (r = 3-5°); Fig. 19, T_c (r = 0-3°), T_e (r = 3-5°);

Fig. 20, T_c (r = 0-3°), T_e (r = 5-7°); Fig. 21, T_c (r = 0-3°), T_e (r =

3-7°)].
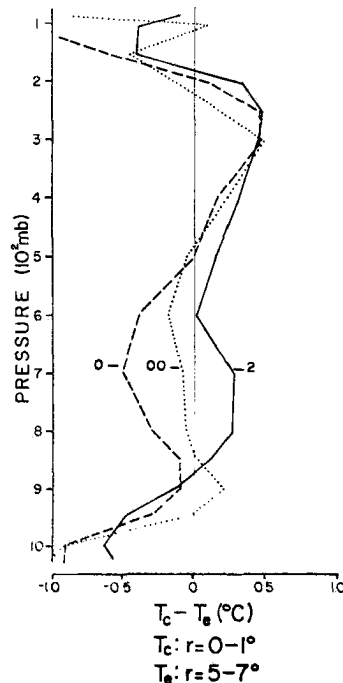
Fig. 17. Cluster (c) minus environment (e) vertical temperature
profiles: pre-typhoon cluster (2) versus non-developing
clusters (0 and 00). T_c = mean temperature of the cluster.
T_e = mean temperature of the surrounding region. T_c:
r = 0-1°, T_e = 5-7°.
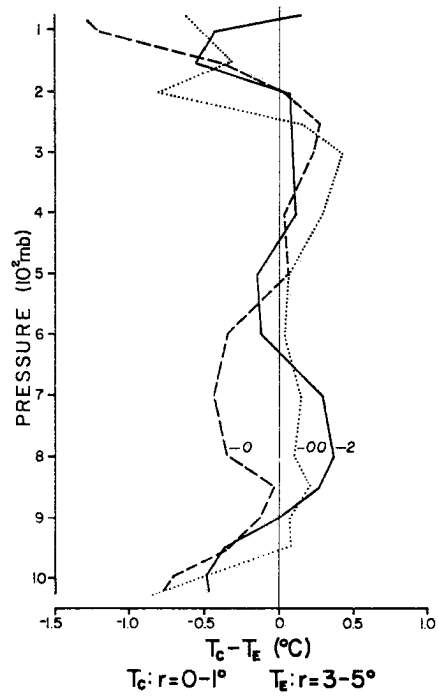
Fig. 18. Same as Fig. 17, except T_c: $r = 0$-1°, T_e: $r = 3$-5°.
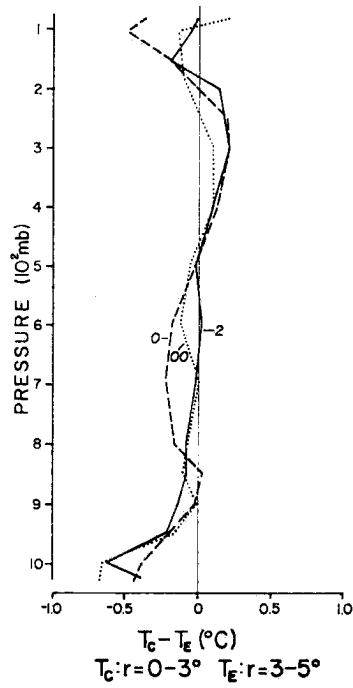
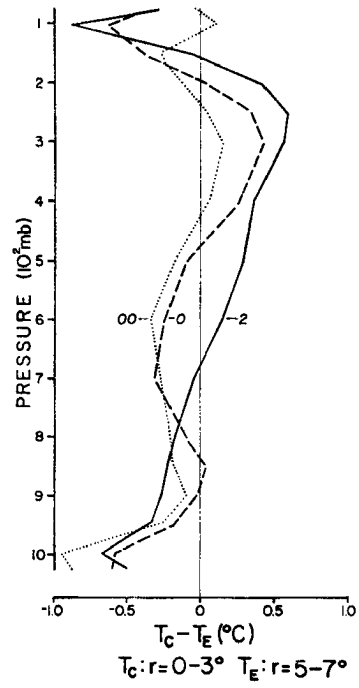Fig. 19. Same as Fig. 17, except T_c: $r = 0$-3°, T_e: $r = 3$-5°.

Fig. 20. Same as Fig. 17, except T_c: r = 0-3°, T_e: r = 5-7°.
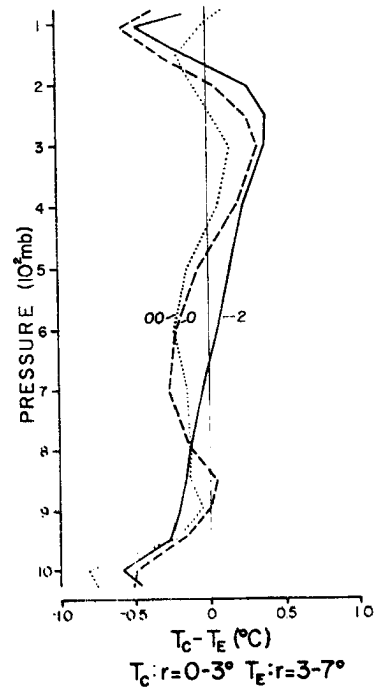

Fig. 21. Same as Fig. 17, except T_c: r = 0-3°, T_e: r = 3-7°.

In general, the temperature profiles and the vertical profiles of mean tangential wind in Figs. 15-16 are well related. Both the pre-typhoon clusters and the non-developing clusters are warm-core in the middle to upper troposphere (500 mb to 200 mb). In general, both cluster systems are cold-core near the tropopause and in the lowest 100 mb. However, in the 600-800 mb layer the non-developing clusters are colder than the surrounding region, while the pre-typhoon clusters are slightly warm-core. This appears to be one of the most fundamental differences between pre-typhoon and non-developing clusters. The 600-800 mb cold-core feature of non-developing clusters is indicated by most of the vertical temperature profiles (Figs. 17-21) and by the tangential wind profiles (Figs. 15-16).

Undoubtedly, an important feature of the typhoon genesis process is the elimination of this 600-800 mb cold-core structure, or the formation of a pre-typhoon cluster which initially does not possess this cold-core. Riehl (1948, 1954, 1969) and Yanai (1961a, 1964) have emphasized the observed cold-core structure of tropical disturbances which do not intensify into tropical cyclones. The composited data indicate that even in the earliest stages the pre-typhoon clusters are slightly warm-core in the 600-800 mb layer. Therefore, it appears that a cold-core system is seldom transformed into a warm-core system which develops into a tropical cyclone, but rather the pre-typhoon cluster lacks a 600-800 mb cold-core structure from the very beginning. If this proves to be correct, then tropical cyclone genesis may be specified more by the initial flow characteristics than by the evolutionary nature of the flow.

3.7 Water Vapor Vertical Profiles

The water vapor mixing ratios within the cluster show small but likely significant differences in the middle levels. The non-developing clusters are drier in 500-900 mb layers by a mean value of 0.5 - 1.0 g Kg^{-1}. Figure 22 depicts the differences in mixing ratio between the pre-typhoon (Stage 2) data and the non-developing (Stages 0 and 00) data within the cluster area (r = 0-3°). Note that the slightly drier layer of the non-developing clusters correspond to the cold-core layers in the thermal structure. This suggests that the cold core is related to moist processes. A more detailed discussion follows in Section 5.

3.8 Zonal Wind Profiles and Propagation Speeds

The vertical shear of zonal wind (u) is portrayed in Fig. 23. The mean u-component of the wind in the cluster region (r = 0-3°) is plotted along with the mean u-component of the propagation vector. The mean meridional wind (v) in the r = 0-3° area is small and propagation is predominantly to the west. Therefore, the difference between the zonal wind and the westward propagation speed is a good approximation of the relative flow of air through the disturbance, or ventilation. The concept of ventilation and its role in extracting heat and moisture from within the clusters area is discussed in Section 5.

Figure 24 shows vertical profiles of u_m (relative zonal wind) averaged within radius 3°. The cluster propagation vector was subtracted from the observed winds for each individual sounding. The relative u-components (u_m) were then composited. Both Figs. 23 and 24 indicate that the non-developing clusters have larger differences between the zonal wind and the westward cluster movement at nearly all levels in the troposphere. According to the mean wind profiles, the non-developing
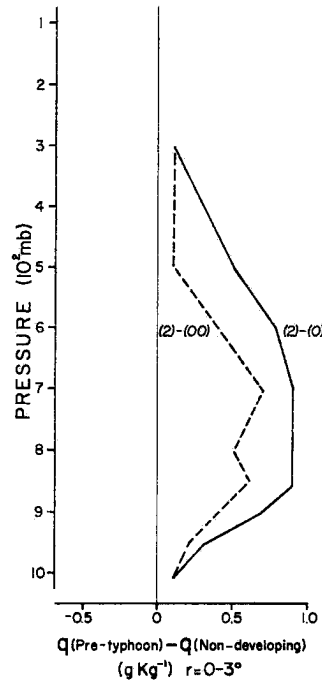
Fig. 22. Differences in water vapor mixing ratio, q, in the r = 0-3°
area between the Stage 2 (pre-typhoon cluster) and Stages 0
and 00 (non-developing cluster). The nighttime (12Z) ob-
servations were used to avoid solar radiation induced errors
in humidity measurements.

clusters are predominantly ventilated from front to back.

Gray (1968, 1975) has previously stressed the importance of small

vertical wind shear as a favorable factor in tropical cyclone genesis.

The "Pre-typhoon" (Stage 2) cluster possesses practically no vertical

zonal wind shear between 150 and 600 mb. The vertical shear of the

non-developing cluster data sets (0 and 00) is larger but still rela-

tively small.

It is interesting to note that data sets 0 and 00 indicate shears

with differing signs in the upper troposphere. Since Stage 00 is a

subset of Stage 0, many of the additional clusters included in data set
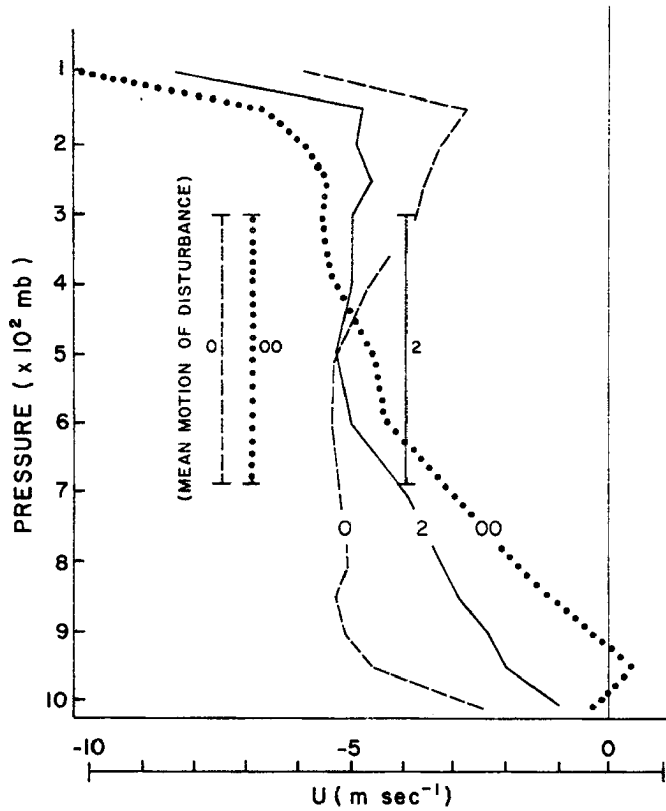
Fig. 23. Zonal wind or u-component of the wind. The mean values of u in the $r = 0^\circ - 3^\circ$ region are plotted for the pre-typhoon (2) and non-developing (0 and 00) clusters. The mean u component of the propagation vector is also depicted.
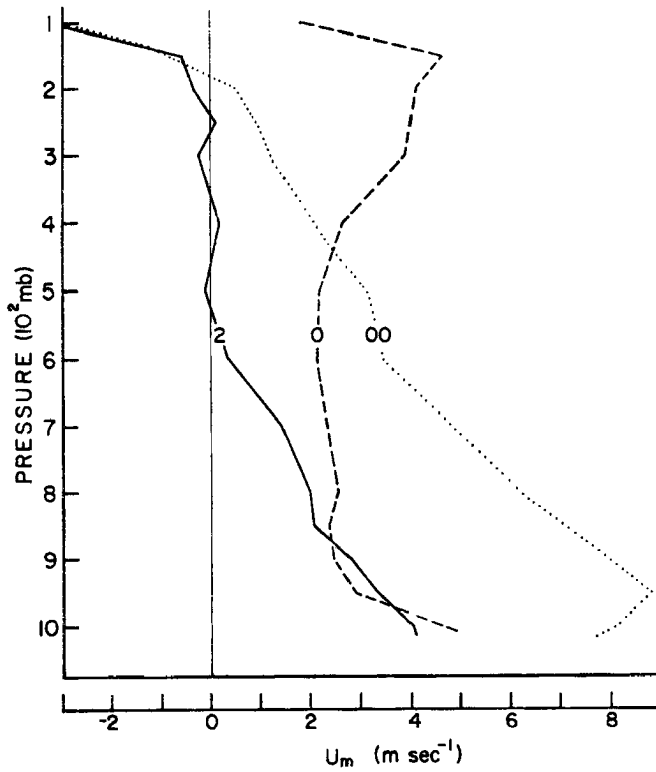

Fig. 24. Vertical profile of (u_m), or the relative zonal wind, averaged in the $r = 0^\circ - 3^\circ$ area. The propagation vector was subtracted from the observed wind for each individual sounding before the (u_m) values were composited.

0 apparently have weaker easterlies and possibly even westerlies in the upper troposphere. The vertical u-profile in Fig. 24 for data set 0 is an average of a large number of zonal wind profiles with considerable variability. Apparently doldrum trough non-developing clusters are ventilated most strongly in the lower and middle troposphere while the non-developing clusters embedded in the easterlies are ventilated most in the upper troposphere. Both the vertical shear of the zonal wind and the previously discussed low-level flow pattern of non-developing clusters are variable features in contrast to the more consistent features such as vertical temperature profiles and mean vertical motion.

A small difference in the speed of cluster movement was noted. Non-developing clusters propagate at a mean speed of about 7 m/sec while the pre-typhoon clusters travel at approximately 5.5 m/sec. The direction is typically to the west or west-northwest. All three cluster data sets have very similar zonal winds at the middle levels (400-700 mb). These are generally accepted to be the "steering levels". The non-developing clusters apparently are propagating slightly faster than this flow. The speed of propagation is a contributing factor to the magnitude of the flow through the cluster (ventilation). The concept of ventilation is thoroughly discussed in Section 5.

3.9 Anticyclonic Outflow and Relative Angular Momentum

Although the magnitudes and heights of the outflow are similar, the basically anticyclonic flow pattern shows some differences as indicated by the 200 millibar analyses in Fig. 25. The pre-typhoon cluster has a more intense outflow channel to the north, while most of the outflow in the non-developing clusters is channeled to the southwest. Mean tangential winds out to 6° radius are listed in Table 8. In general, the
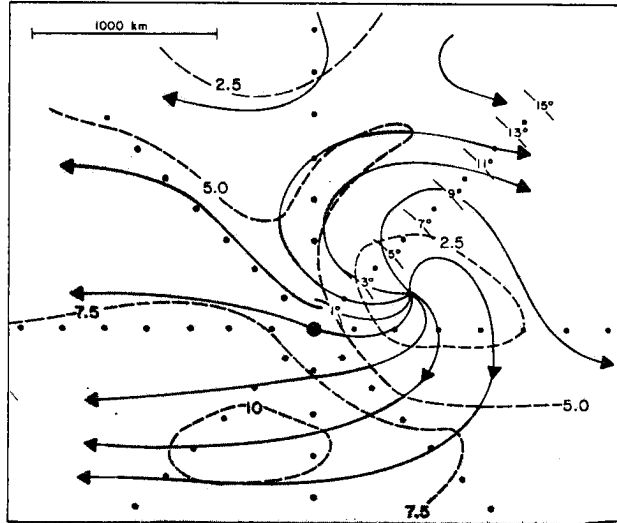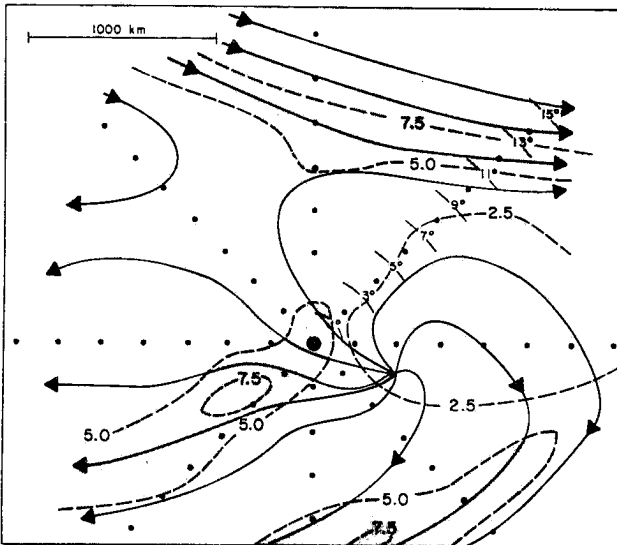
Pre-typhoon cluster
(Stage 2)
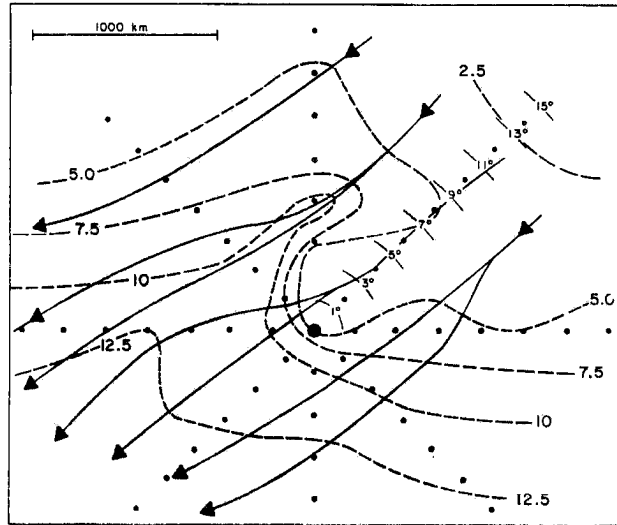
Non-developing cluster
(Stage 00)

Non-developing cluster
(Stage 0)

Fig. 25. 200-mb streamline and isotach analyses (m sec^{-1}).

TABLE 8

Mean Tangential Wind at 200 mb
$(m\ sec^{-1})$

Data Set	$r = 2^{\circ}$	$r = 4^{\circ}$	$r = 6^{\circ}$
Non-developing (Stage 00)	-1.35	-1.95	-1.09
Non-developing (Stage 0)	-0.70	-0.66	-1.25
"Initial" (Stage 1)	-1.77	-1.86	-2.84
"Pre-typhoon" (Stage 2)	-1.18	-1.72	-2.90

pre-typhoon cluster circulations are more anticyclonic (negative tangential wind) than are those of the non-developing clusters at all distances out to 6° radius at 200 mb.

The 200 mb relative vorticity analyses are depicted in Fig. 26. A basic difference between the non-developing cluster (Stage 00) and the pre-typhoon cluster (Stage 2) appears in the vorticity pattern to the north of the clusters. The pre-typhoon cluster has an area of negative relative vorticity out to 7° to the north. The Stage 00 non-developing cluster composite has positive relative vorticity to the north and northwest. This feature is not evident in Stage 0 non-developing data set.

These features of the composited wind data support the evaluation by Sadler (1974) of the favorable upper tropospheric features for typhoon development and intensification. Sadler observes that developing disturbances typically possess an upper level "outflow channel". He suggests that the tropical upper tropospheric trough (TUTT) supplies
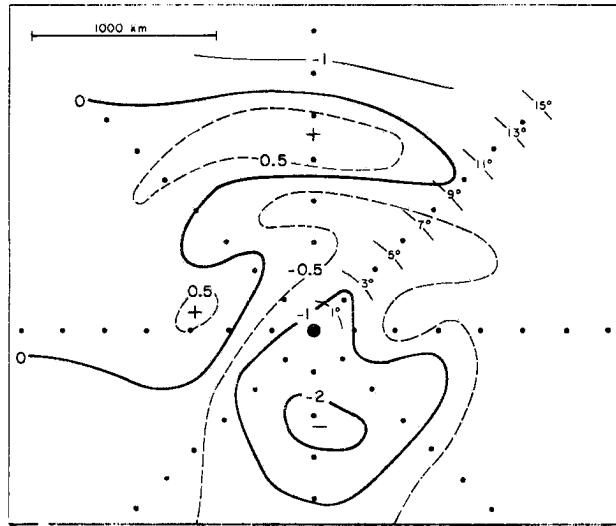
Pre-typhoon cluster
(Stage 2)
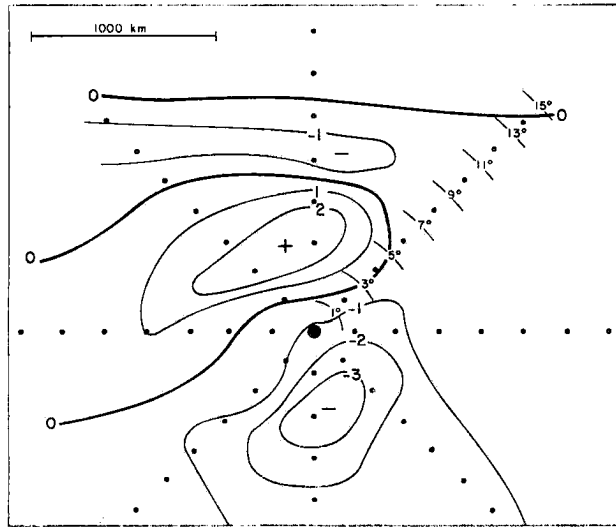
Non-developing cluster
(Stage 00)
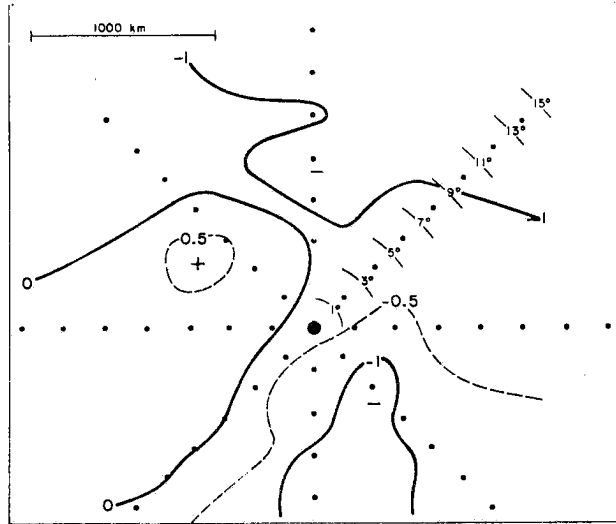
Non-developing cluster
(Stage 0)

Fig. 26. 200-mb relative vorticity ($10^{-5}\mathrm{sec}^{-1}$) analyses.

the "outflow channel" for low-latitude intensifying and developing disturbances.

The physical reasoning for an "outflow channel" being a favorable feature for typhoon genesis and intensification cannot be the removal of excess heat from the disturbance region. Heat accumulating in the upper troposphere near the disturbance is favorable for intensification since surface pressure decreases in response to upper level warming. The "outflow channel" may likely be important in increasing the export of negative relative angular momentum from the upper circulation. This acts to increase positive relative angular momentum within the system.

Relative angular momentum with respect to the cluster center is defined as $\overline{V}_T r$, the product of the tangential wind (V_T) and the radial distance (r) to the cluster center. Figure 27 depicts the total (mean and eddy) transport of relative angular momentum at 4° radius for the non-developing cluster, pre-typhoon cluster and intensifying tropical depression. The import of relative angular momentum is much larger both in the lower troposphere and in the outflow layer with the pre-typhoon cluster compared with the non-developing cluster. The transports were computed by calculating the product of V_R and V_T for each sounding and compositing within the $r = 3-5^o$ region. Therefore, the total transport ($\overline{V_R V_T r}$) terms contain both a mean ($\overline{\overline{V}_R \overline{V}_R r}$) and an eddy ($\overline{V_R' V_r' r}$) transport. The precise effects of these transports on the cluster circulation cannot be evaluated without performing a thorough angular momentum budget analysis. This was beyond the scope of this study.

It is noted that the total import of positive relative angular momentum ($V_R V_T r$ integrated around the cluster) is a function of the mean tangential wind, mean radial wind, and "eddy" circulation. In the inflow
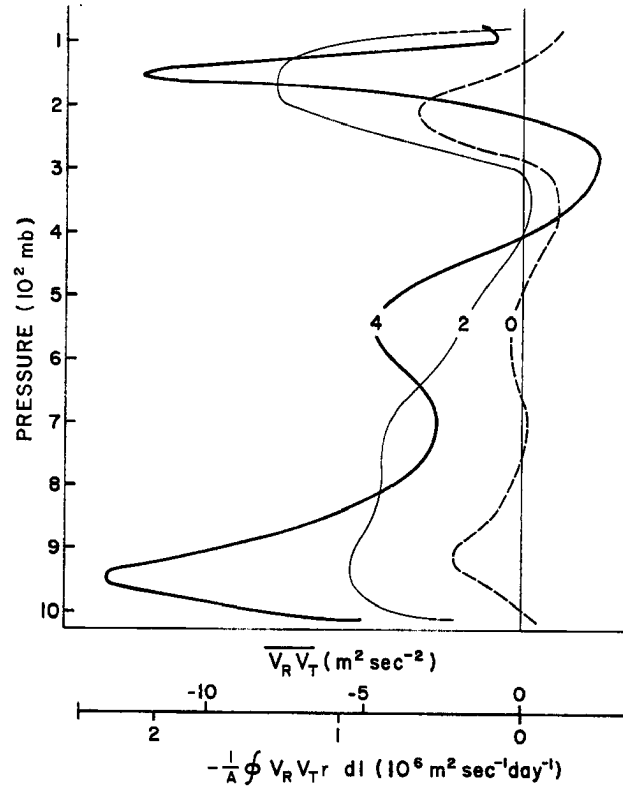
Fig. 27. Transport of relative angular momentum at r = 4° for Stage 0
(non-developing cluster), Stage 2 (pre-typhoon cluster) and
Stage 4 (intensifying tropical depression). The $V_R V_T$ pro-
ducts for the individual soundings in the r = 3-5° radial
band were composited so that the transports represent the sum
of the mean and eddy motions.

layers where the tangential wind is positive, the difference is approx-
imately proportional to the difference in cyclonic flow. In addition,
the more anticyclonic character of the pre-typhoon cluster's outflow
exports more negative relative angular momentum than with the non-
developing cluster. The net effect is a larger import of positive
relative angular momentum in the outflow layer with pre-typhoon clusters.

Wachtmann (1968) investigated the role of angular momentum trans-
ports in tropical storm dissipation over warm tropical oceans. He
found the deficiency of inward angular momentum transport to be a
primary factor in tropical storm dissipation based on several case
studies.

3.10 Summary

The differences between a pre-typhoon cloud cluster and a non-developing cluster revealed by the composited rawinsonde data are summarized:

1) low-level vorticity - - The relative vorticity is about two times greater with the pre-typhoon clusters in the lower troposphere.

2) the maximum mean vertical velocity within an 8° diameter region centered on the clusters is about 25% greater with the pre-typhoon clusters.

3) vertical temperature structure at 500-800 mb - - Pre-typhoon clusters are warm-core. Non-developing clusters are cold-core.

4) vertical profiles of relative mean zonal wind - - The difference between the mean westward cluster movement and the mean zonal wind speed is smaller with the pre-typhoon clusters through most of the troposphere.

5) speed of propagation - - Pre-typhoon clusters propagate slower.

6) anticyclonic outflow - - The outflow is more anticyclonic with pre-typhoon clusters.

7) The import of relative angular momentum is significantly larger with the pre-typhoon clusters.

8) water vapor - - The pre-typhoon clusters possess slightly greater quantities of water vapor.

These differences between non-developing and pre-typhoon clusters probably represent very significant key parameters in specifying whether or not typhoon genesis will occur.

4. OBSERVED INTENSIFICATION OF THE TYPHOON AT INNER-CORE RADII

The results of the data composites at the different stages of
development from a pre-typhoon cloud cluster to a typhoon are discussed
below for the important inner-core region (center to 2° radius).

4.1 Divergence and Vertical Motion

The vertically integrated $1-3^{\circ}$ radius radial wind indicated too
much net divergence between the surface and 100 mb. To allow for a mass
balanced vertical profile of radial wind the abscissa is shifted to the
right. In the early stages of 1 and 2 0.2-0.3 m/sec had to be added to
each $1-3^{\circ}$ radial wind such that a surface-100 mb mass balanced vertical
profile was obtained. This magnitude of correction did not have to be
made in the later stage samples of Frank (1976) or the other tropical
cloud cluster compositing studies of this project. This lack of close
balancing is believed to result from the smaller $1-3^{\circ}$ radius rawinsonde
data sample (151 cases) and more difficult position problems at inner
core radii. Despite this required 0.2-0.3 m/sec correction to the $1-3^{\circ}$
radius radial wind profile we believe the resulting $1-3^{\circ}$ radial wind
profiles are quite representative and will be verified in later more
dense data averages. The resulting $0-2^{\circ}$ radius vertical motion profiles
will now be discussed. These are kinematically derived from the mass-
balanced radial winds at 2° radius from the disturbance centers. The
mean radial winds in the radial band $r = 1-3^{\circ}$ were assumed to represent
the radial winds at $r = 2^{\circ}$.

As intensification takes place, additional convergence becomes
concentrated in the lowest 100 millibars of the planetary boundary layer.
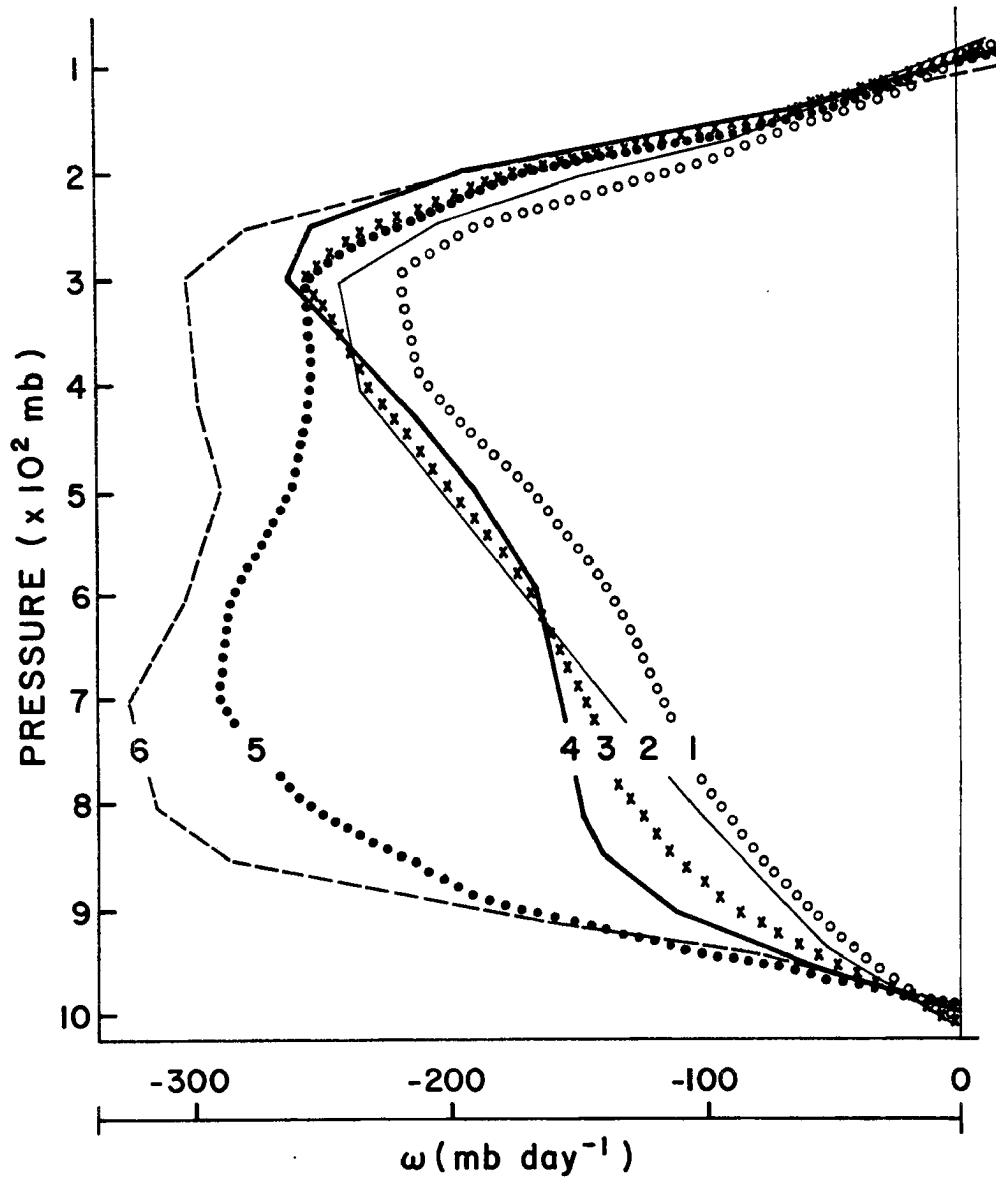Figure 28 portrays the increasing effect of the frictionally forced

Fig. 28. Mean vertical motion (ω) computed from mean radial
wind profiles at radius 2°. The various stages of
development are as follows: 1) "Initial; 2) "Pre-
typhoon"; 3) "Genesis"; 4) "Intensifying"; 5) and
6) from W. Frank's (1976) typhoon data according to
reported central sea-level pressure 5) 980-1000 mb
and 6) 950-980 mb.

boundary layer convergence on the vertical velocity (ω) profiles during
the intensification.

4.2 Relative Vorticity

Vertical profiles of the mean tangential wind in the $r = 1\text{-}3^{\circ}$
radial band for various stages of development are presented in Fig. 29.
These values are approximately proportional to the mean relative vorticity
within 2° radius. Figure 29 indicates that the maximum relative vorticity
is found just above the boundary layer and that negative relative vor-
ticity is present in the upper troposphere. This is true for all stages
of development from a pre-typhoon cluster to a typhoon.

4.3 Tropospheric Warming

As the pre-typhoon cloud cluster develops into a tropical depres-
sion and eventually a typhoon, the entire troposphere except for the
lowest and highest levels shows a significant warming. As a result
surface pressures fall, and tangential winds consequently increase.
Figure 30 indicates that these changes are well correlated.

It is observed that above the tropopause, which is at about 110 mb,
the circulation is not significantly influenced by the circulation below.
Therefore, there must be a level in the stratosphere at which geopoten-
tial heights are not effected by temperature changes induced by the
synoptic-scale disturbances below. Table 9 lists the observed changes
in geopotential thickness for individual pressure layers within a mean
cluster area ($r = 0\text{-}3^{\circ}$) which take place from Stage 2 to Stage 4. The
temperature changes revealed by the composited data have been converted
to thickness changes assuming hydrostatic conditions. These calculated
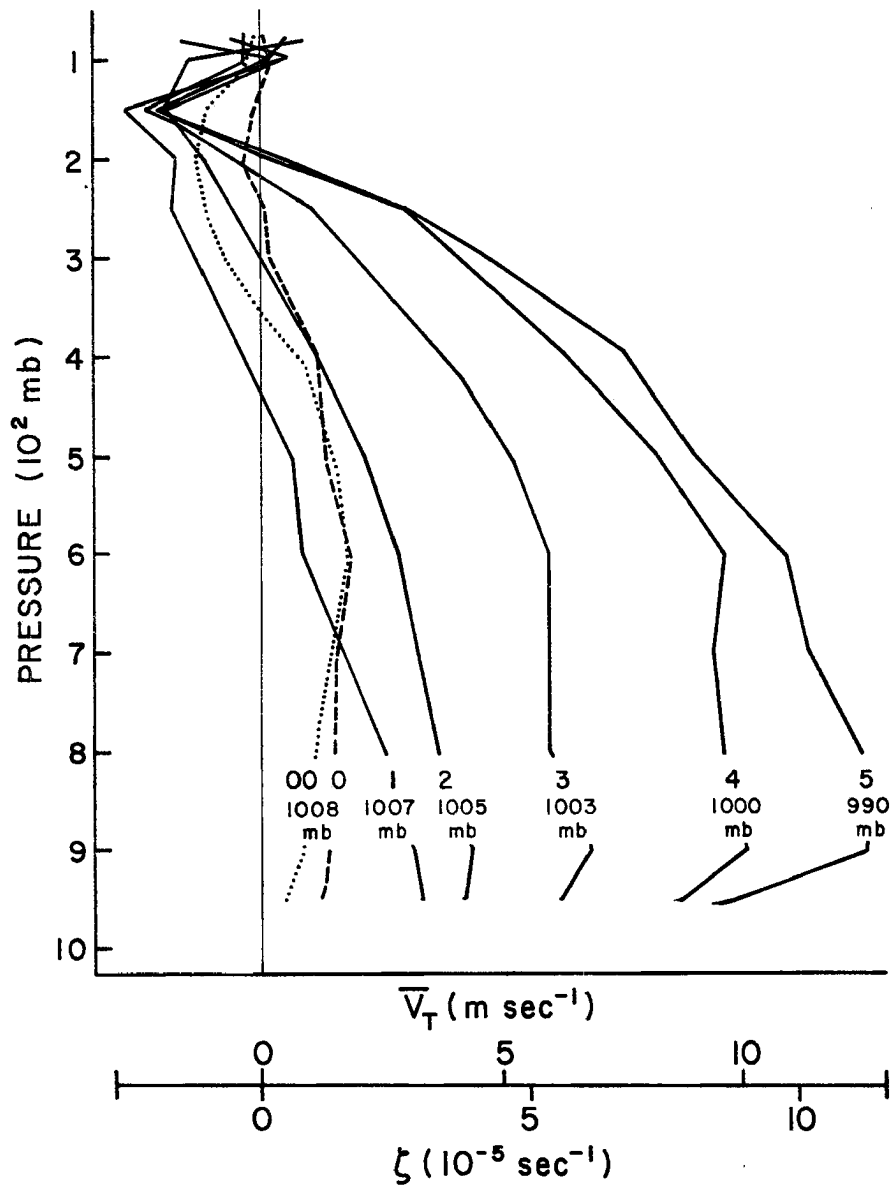thickness changes, also listed in Table 9, correspond well with the

Fig. 29. Vertical profiles of mean tangential wind at r = 2° for various data sets. (0 and 00) non-developing cloud clusters; 1) "Initial"; 2) "Pre-typhoon; 3) "Genesis"; 4) "Intensifying"; 5) W. Frank's (1976) typhoon data with central pressure, 980-1000 mb. Note that these values can be interpreted as representative of the mean relative vorticity within radius 2°, with values as shown in units of 10^{-5} sec^{-1}. The best estimate of the central sea-level pressure at each stage is given.
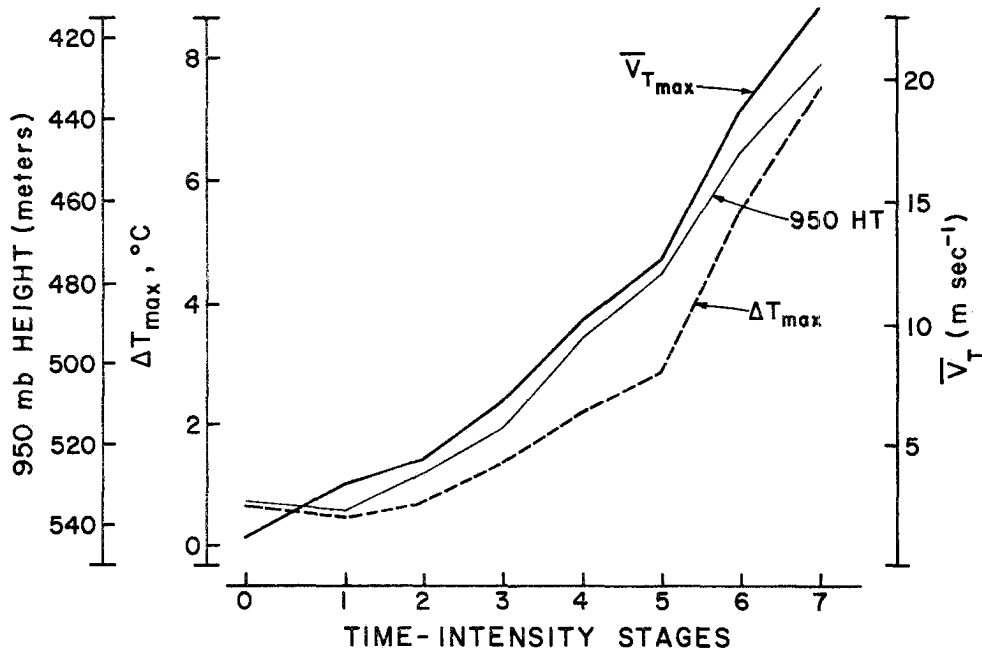
Fig. 30. Corresponding trends of tangential wind, surface pressure, and strength of warm core during typhoon genesis and intensification. $V_{T_{max}}$ is observed at $r = 2^{\circ}$ and the level where it is maximum, typically near 900 mb. The 950 HT, the geopotential height at 950 mb in the $r = 0-1^{\circ}$ area, is analagous to surface pressure. ΔT_{max} is the temperature at $r = 0-1^{\circ}$ minus the temperature at $r = 5-7^{\circ}$, at the level where this difference is maximum, usually near 250 mb.

observed changes. Both columns of thickness changes, when integrated from 80 mb to 950 mb, indicate that the inner 2° radius mean height change at 950 mb is about 20 meters or 2 mb. The low-level pressure changes and integrated thickness changes below 80 mb agree quite well. Therefore, it is assumed that changes in meteorological parameters above the 80-millibar level are relatively unimportant and probably unrelated to tropical cyclone genesis. The zonal wind flow at 70 and 80 mb about the disturbance as it develops also support this assumption.

The maximum tangential winds increase in direct proportion to the 950 mb heights or surface pressures as depicted in Fig. 30. Since the

TABLE 9

Comparison of Observed Temperature and Pressure Thickness Changes to
Computed Pressure Thickness Changes Within the $r = 0\text{-}3^{\circ}$ Area from
Stage 2 to Stage 4

Pressure Layer (mb)	Temperature Change $T_4\text{-}T_2$ ($^{\circ}$C)	Height Change-Hydrostatic Computation	$Z_4\text{-}Z_2$ (meters) Observed From the Composited Data
80-100	-.98	-6.38	-5.00
100-150	-.09	-1.05	.85
150-200	.61	5.11	4.80
200-250	.75	4.88	3.90
250-300	.75	4.00	3.90
300-400	.65	5.44	4.72
400-500	.65	4.23	5.20
500-600	.66	3.52	3.43
600-700	.55	2.48	1.65
700-800	.37	1.45	1.20
800-850	.18	.32	.50
850-900	.03	.05	-.65
900-950	-.01	-.02	-.55
950-1000	-.05	-.08	-2.95

Observed Height Changes:			
		950 mb	-19.9 ($\sim$2 mb)
		1000 mb	-19.0 ($\sim$2 mb)

57

surface pressure is determined by the vertical temperature profile
according to hydrostatic considerations, the process of tropospheric
warming is a fundamental feature of the genesis process.

The difference between the mean temperature ($r = 0-1^{\circ}$) within the
cluster, T_c, and that of the surrounding region ($r = 5-7^{\circ}$), T_e, is
shown in Fig. 31 for various stages of development. Figure 32 depicts
the cluster and surrounding region temperature difference where T_c is
represented by the $r = 0-3^{\circ}$ area and T_e by the $r = 3-7^{\circ}$ area. Note
that the warm-core structure is maximum in the 200-300 millibar layer
for all stages of development. This is at a slightly higher level than
the 400 mb warm core maximum indicated by case studies of Yanai (1961a,
1964). A cold-core disturbance exists only near the surface (heat is-
land) and near the tropopause. Warming occurs throughout a large depth
of the atmosphere and is maximum at and just below the outflow layer.
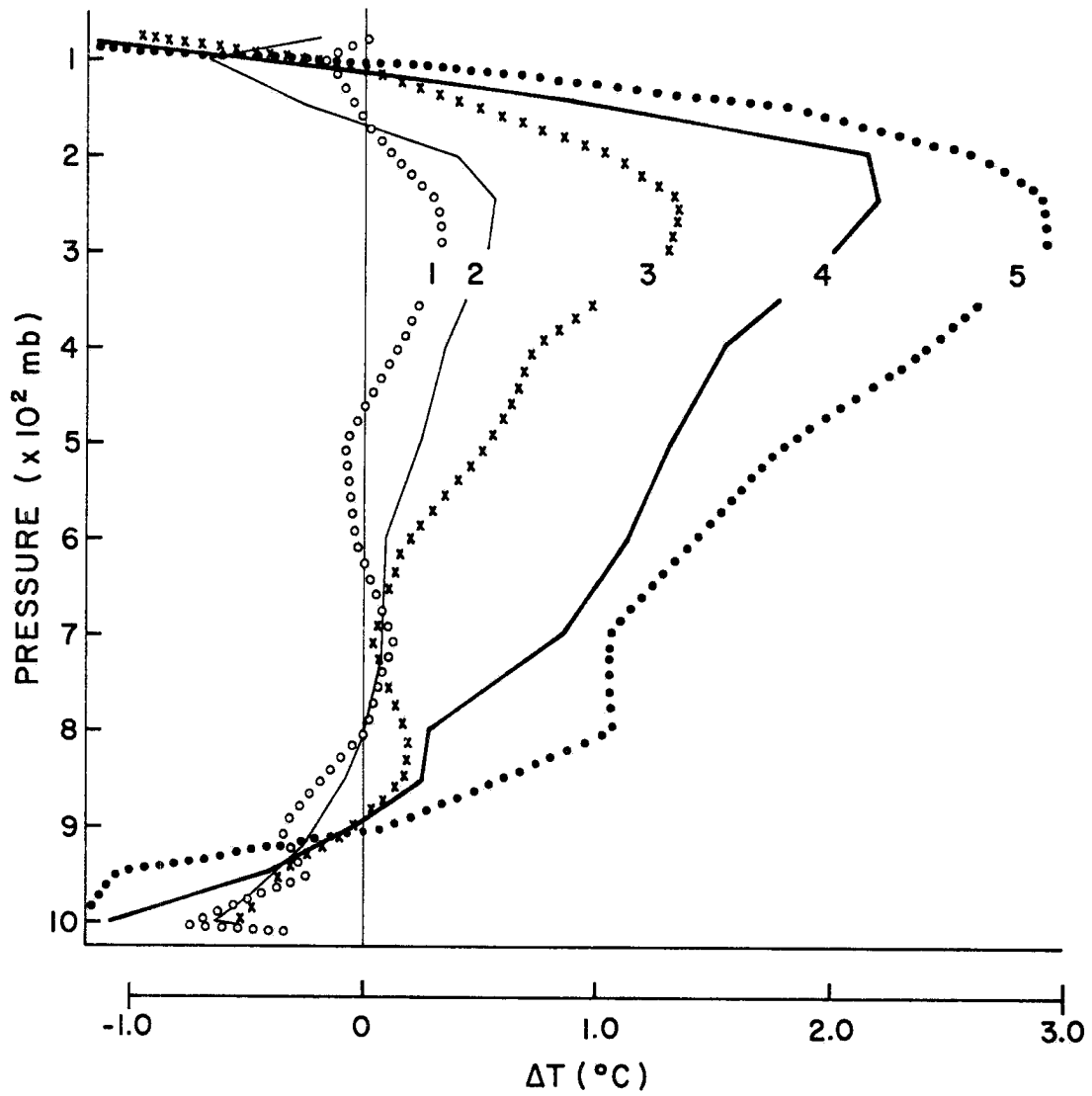
Fig. 31. Vertical profiles of ΔT. $\Delta T = T_c$ ($r = 0\text{-}1^{\circ}$) minus T_e ($r = 5\text{-}7^{\circ}$). The data sets are: 1) "Initial"; 2) "Pre-typhoon"; 3) "Genesis"; 4) "Intensifying"; 5) "980-1000 mb central pressure), (W. Frank, 1976).
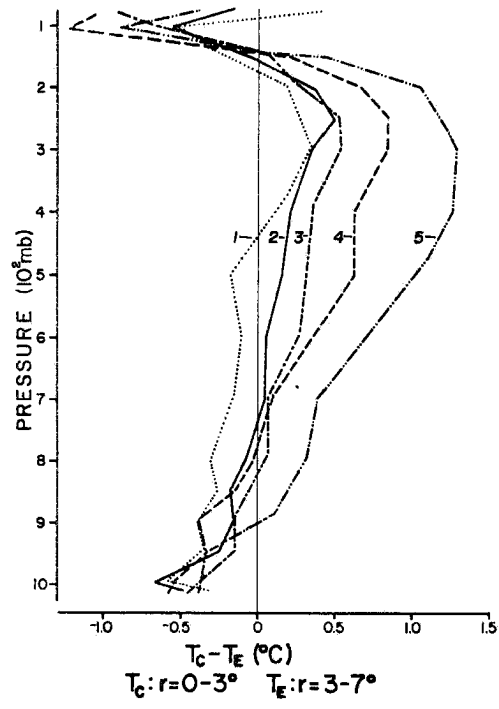
Fig. 32.   Same as Fig. 31 except T_c: $r = 0-3^{\circ}$, and T_e: $r = 3-7^{\circ}$.

5. VENTILATION AND TROPOSPHERIC HEATING

The importance of ventilation or "blow-through" as an inhibiting

mechanism in tropical cyclone genesis has been proposed and discussed

by Gray (1968, 1975) and Lopez (1968). It has been shown that tropical

cyclone formation is accompanied by a decrease in surface pressure which

is a response to tropospheric warming. A progressive accumulation of

temperature in a deep vertical column in the troposphere is a necessary

condition for genesis. What is the role of ventilation or the relative

flow of air through the cluster in preventing the accumulation of upper

level temperature in the non-developing disturbances? This process will

now be discussed for the 0-4° radius (8° diameter) broader disturbance

circulation.

5.1 Ventilation

Ventilation is defined here as the relative non-divergent flow

through the disturbance. The composited wind data allow this feature to

be studied. The mean relative radial winds (disturbance motion subtracted

out) are used to evaluate the ventilation as well as the divergent compo-

nent of the relative flow.

The relative radial winds, V_{Rm}, averaged at the eight locations or

"sectors" around the disturbance 4° radius circle are used in the compu-

tations. The mean wind within the r = 3-5° radial band in each sector is

assumed representative of the wind at r = 4° in that sector. The average

absolute value of the relative radial wind at the disturbance perimeter is

denoted $\overline{|V_{Rm}|}$ and is referred to as the "total" relative flow. It is

computed as 1/8 $\displaystyle\sum_{i}^{8} \left|V_{Rm_i}\right|$ where V_{Rm_i} is the relative radial

wind averaged for a given sector at $r = 4^{\circ}$. The algebraic mean of the eight sector relative radial winds, $\overline{V_{Rm}}$, represents the divergent component of the flow and in fact can be directly converted to a divergence (time^{-1}) value, as follows:

$$\frac{1}{A} \oint V_{Rm} \; dl = \frac{2\pi r}{\pi r^2} \; \overline{V_{Rm}} = \frac{2\overline{V_{Rm}}}{r} = DIV$$

where   A   = disturbance area,
               dl = segment of the perimeter,
               r   = cluster radius

The difference between the total relative flow and the absolute value of the divergent flow defines the non-divergent flow, or ventilation (VEN). Thus,

$$\begin{array}{ccccc} \text{VEN} & = & \overline{\left|V_{Rm}\right|} & - & \left|\overline{V_{Rm}}\right| \\ \text{(non-divergent)} & & \text{(total)} & & \text{(divergent)} \end{array}$$

where $|\;\;|$ indicates the absolute value of the quantity, and $\overline{\quad\quad}$ represents the mean value of the eight sector values. A simplified hypothetical example of this computation is depicted in Fig. 33.

The vertical profiles of these computations for the "Pre-typhoon" (Stage 2) and non-developing (0 and 00) data sets are plotted in Fig. 34. Significantly more total relative flow is observed with non-developing cloud clusters. Most of this is due to the differences in ventilation, or the non-divergent blow-through wind component as depicted in Fig. 35.
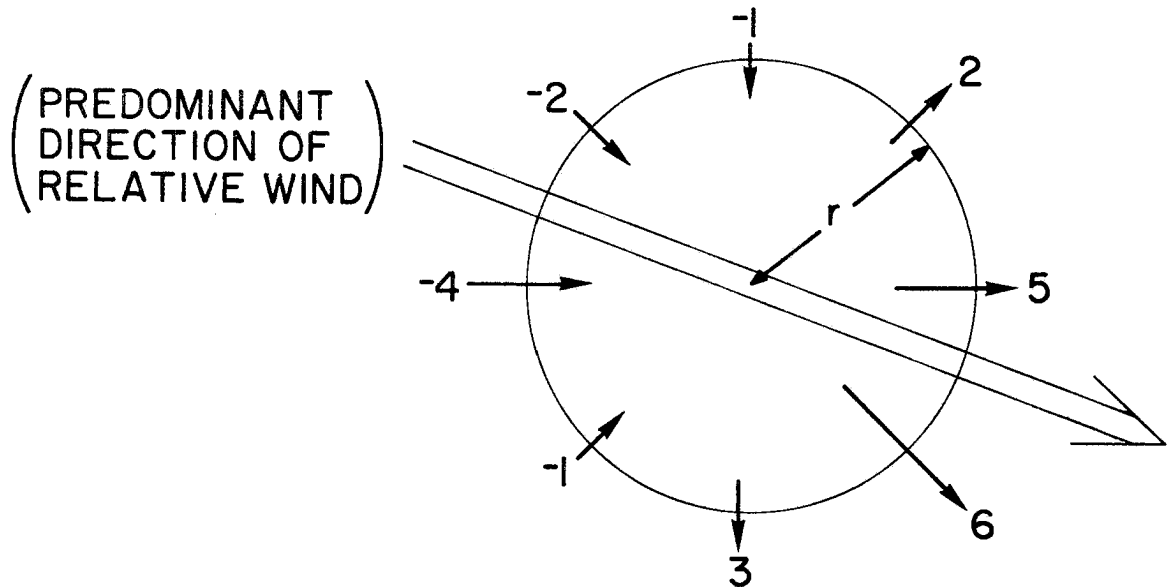
Computations are as follows:

$$(\text{total}) = \quad \overline{|V_{Rm}|} = \frac{\sum |V_{Rm}|}{8} = \frac{24}{8} = 3$$

$$(\text{divergent}) = \left|\overline{V_{Rm}}\right| = \left|\frac{\sum V_{Rm}}{8}\right| = \frac{8}{8} = 1$$

$$(\text{non-divergent}) = \text{VEN} = (\text{total}) - (\text{divergent}) = 3 - 1 = 2$$

$$(\text{total}) = (\text{divergent}) + (\text{non-divergent})$$

$$\overline{|V_{Rm}|} = \left|\overline{V_{Rm}}\right| + \text{VEN}$$

$$3 = 1 + 2$$

Fig. 33. A hypothetical example of the evaluation of $\overline{|V_{Rm}|}$, $\left|\overline{V_{Rm}}\right|$ and VEN. The mean relative radial winds, V_{Rm}, are depicted at the eight locations around the $r = 4°$ cluster perimeter. Inward radial winds are negative. Units are meters per second.
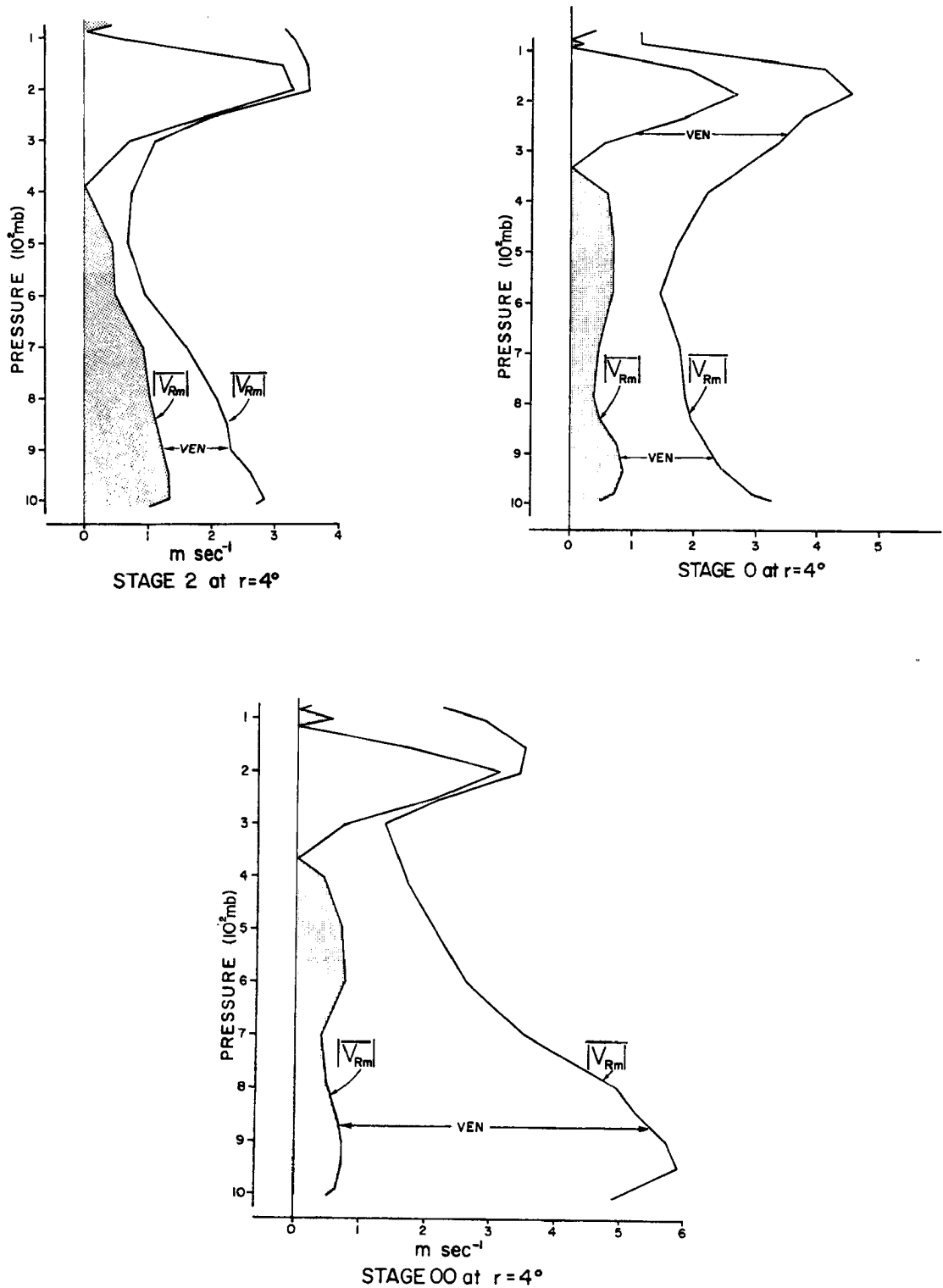
Fig. 34. Vertical profiles in m/sec of the total mean relative flow'($\overline{|V_{Rm}|}$), the divergent ($|\overline{V_{Rm}}|$), and non-divergent (VEN) portions of the flow. Computations are based on the mean relative radial winds at 4° radius. The data sets are: 2, "Pre-typhoon"; 0, non-developing cluster (general); 00, non-developing cluster (restricted).
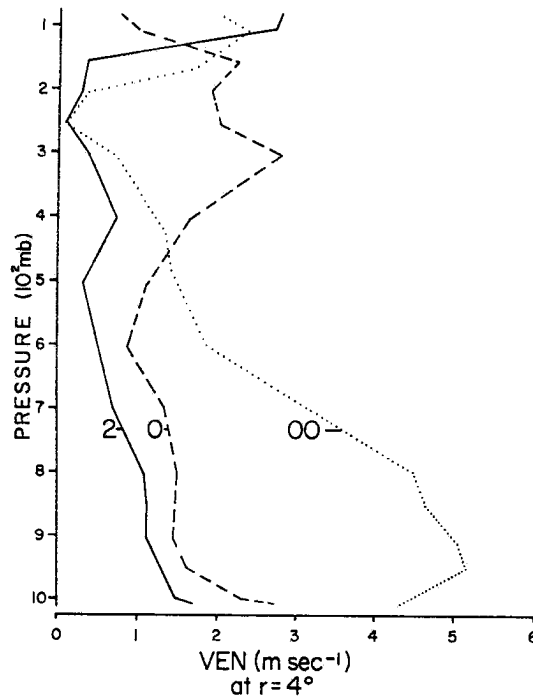
Fig. 35. Ventilation (VEN) or non-divergent mean relative flow at radius 4° for the pre-typhoon (Stage 2) and non-developing (0 and 00) disturbances.

The ventilation integrated through the troposphere is considerably larger with both non-developing disturbance data sets compared with the pre-typhoon disturbance. However, the Stage 00 data shows the largest differences from the Stage 2 data in the lower and middle troposphere, while ventilation in the upper troposphere is not significantly different. With Stage 0, differences from Stage 2 are small in the lower troposphere and large in the upper troposphere. These features are a reflection of the previously discussed (Section 3.8) differences between data sets 00 and 0 with regard to the vertical shear of the zonal wind. This analysis suggests that relatively small values of ventilation through the entire depth of the troposphere and not just in the maximum warm-core levels are characteristic of pre-typhoon clusters.

To evaluate the effects of ventilation on the disturbance, the "inner core" to "environment" temperature gradients must be considered. At levels where the system is cold-core, ventilation acts to warm the inner core, while cooling due to ventilation occurs at warm-core levels. Regardless of the direction of the relative radial flow, it will act to reduce the temperature gradient between the cluster and the surrounding region.

More importantly, ventilation of water vapor acts to reduce the inner core moisture values, and requires that more evaporation occur for moisture maintenance. This leads to more cooling of the cluster. Thus, the large OO data set lower tropospheric ventilation is likely a strong inhibiting influence to development.

5.2 Disturbance Heat Sources

Several physical processes can be identified which heat or cool the disturbance with respect to its environment. Ventilation always acts to reduce the magnitude of the warming or cooling which hydrostatically effect the surface pressure beneath the cluster. Because clusters are generally more moist than their environmental regions, ventilation typically acts to dry the cluster and induce larger evaporational cooling.

The vertical mass recycling associated with cumulus and cumulonimbus convection is a potential cluster heat source. Latent heat of condensation is released in actively growing cumulus and cumulonimbus clouds. As discussed by Gray (1972, 1973) most of this condensation energy is used to maintain cloud buoyancy. Due to detrainment and evaporation of cloud and liquid water, cumulus clouds typically do not result in direct warming of their immediate environment. Latent heat is converted into potential energy which is not realized as a temperature

increase until the compensating subsidence warms the air dry-adiabatically. Some of this compensating subsidence or recycling occurs locally within the cluster and acts to warm the disturbance with respect to the surroundings.

An important cooling process associated with cumulus and cumulonimbus clouds is the evaporation of cloud water and rain water as a result of cloud entrainment and detrainment. Cumulus and cumulonimbus towers which overshoot their level of neutral buoyancy will also contribute to the cluster cooling.

The net radiation, long-wave (infrared) plus short-wave (solar), is another possibly important cluster heat source. Beneath the extensive cluster cirrus shield, net radiation will warm the cluster with respect to surrounding less-cloudy regions. Relatively large cooling occurs at cloud top. The role of radiation is discussed in Section 8.3.

A precise and thorough evaluation of the effects of cumulus convection, radiation, and ventilation on the heat budget of both pre-typhoon and non-developing clusters is desirable, and will be treated in forthcoming research.

Extensive analysis of dry and moist static energy budgets with large data samples are needed. These energy budget analyses using composited data have been performed by W. Frank (1976) with respect to tropical cyclones. A thorough energy budget analyses of non-developing and pre-typhoon cloud clusters is beyond the scope of this study.

6. DISCUSSION

A quantitative comparison of non-developing and pre-typhoon cloud clusters has been made by compositing rawinsonde data. Several differentiating criteria have been revealed and several previous ideas have been reinforced. The findings of this study are presently being integrated with studies at CSU by Arnold (1977) and Erickson (1977) in which special DMSP satellite data since 1971 is being composited with respect to developing and non-developing disturbance clusters. These results will be reported on next year.

6.1 Monsoon Trough and Small Vertical Shear as Favorable Features for Genesis

The equatorial trough region has been identified as the most favorable location for tropical cyclone genesis (Sadler, 1967a, 1967b; Gray; 1968 Fett, 1968). The low level flow pattern associated with the pre-typhoon cluster is indicative of the monsoon (or doldrum) trough with southwesterly winds to the south and easterlies to the north (see Fig. 14). This wind pattern also occurs with many non-developing clusters (Stage 00). However, the mean vertical shears are significantly different. Figure 36 shows the mean zonal wind (u) through the troposphere within the cluster and 6° to the north and south. It is seen that the vertical shear is significantly smaller within the pre-typhoon cluster than in the non-developing cluster (Stage 00). Although the Stage 0 vertical shear is quite weak, this may be the result of smoothing out large individual shears of opposite sign. Previous observational studies (Gray, 1968, 1975; Sartor, 1968) also indicate that small vertical wind shears through a large depth of the troposphere are favorable for tropical cyclone genesis.

68

STAGE 2 (PRE-TYPHOON CLUSTER)

STAGE O (NON-DEVELOPING CLUSTER)

STAGE OO (NON-DEVELOPING CLUSTER)
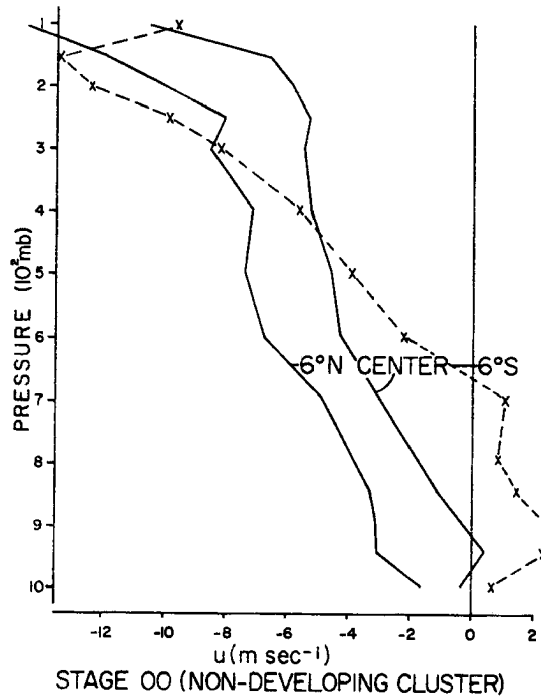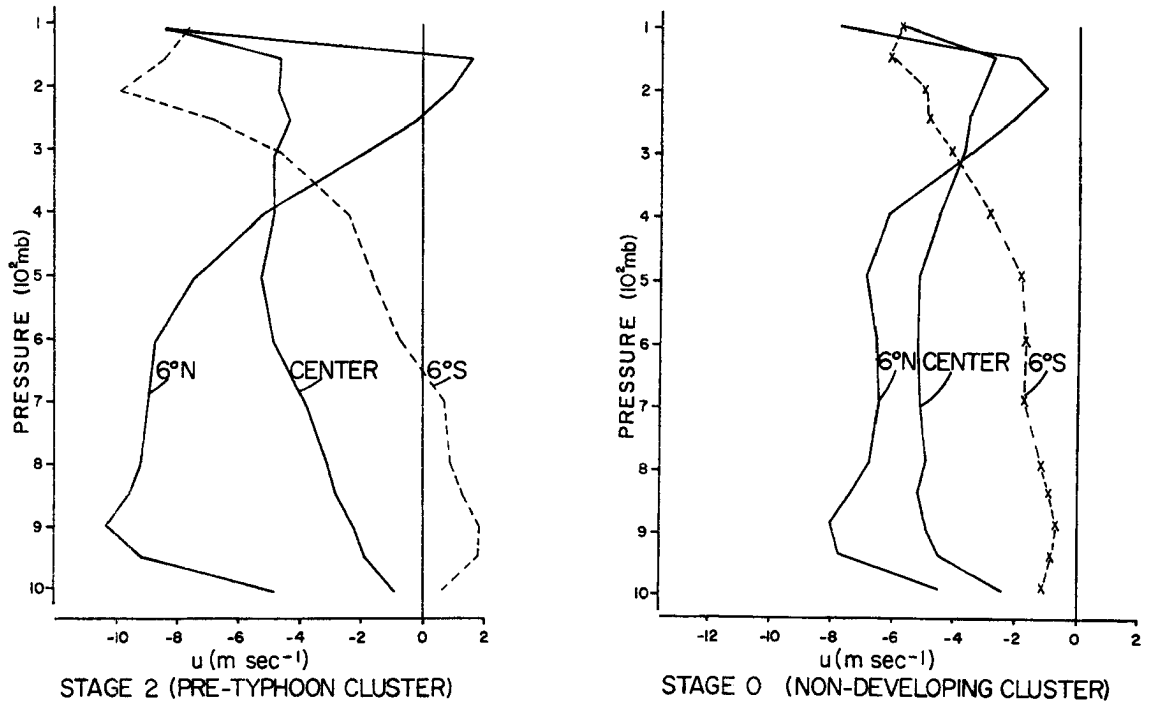
Fig. 36. Mean zonal wind at the cluster center (r = 0-3°), at 6° radius
north (sector 1, r = 5-7°) and at 6° radius south (sector 5,
r = 5-7°) of the cluster center.

The physical reasoning for a small shear environment being favorable for genesis is that it allows for an accumulation of sensible heat and latent energy (water vapor) in a vertical column over a relatively small area. The sensible energy accumulation is important since it will induce a surface pressure decrease and a resulting increase in the import of mass, vapor and angular momentum. The inhibiting of moisture transport out of the cluster by small ventilation is probably even more important than that of sensible temperature.

Analysis of the ventilation is a more direct measure of the effect of a vertically sheared environment on the cluster. The analyses of ventilation in this study support the conclusions and discussion of previous studies by Lopez (1968) and Gray (1968, 1975). Integrated through the troposphere, the ventilation is greater in an environment with a greater vertical wind shear. As the ventilation in the middle and upper troposphere, where sensible heat energy is accumulated, is small, loss of water vapor may be the most important genesis inhibiting process of ventilation.

6.2 Thermal Structure and Heating Functions

Ventilation cannot fully differentiate between a pre-typhoon cluster and non-developing cluster from the accumulation of sensible heat point of view. Since the two cluster systems have cluster-to-environment temperature gradients of different signs in the lower and middle troposphere (500-800 mb), the heating functions must also be fundamentally different at those levels. To maintain the observed cold-core in the non-developing clusters, a cooling in the cluster relative to the environment is necessary. Advection due to ventilation is continually acting to reduce the magnitude of the 500-800 mb cold-core. In the

71

pre-typhoon cluster, a warming mechanism is needed to maintain its
warm-core. Evaporation of detrained cloud and rain water acts to cool
the cluster. Convection induced local subsidence acts to warm. Due to
similarities in cloudiness the net radiation for both systems is likely
to be quite similar. Therefore, it follows that since evaporation is
the only likely differentiating cooling mechanism, the moisture and
water vapor budgets of clusters are quite likely very important genesis
specifying parameters. Assuming similar liquid water contents, the
mean water vapor budget (q) will largely specify the amount of evaporation
which is occurring. The slightly drier characteristic of the non-
developing clusters at 500-800 mb probably results in more evaporation
cooling.

The characteristic deep cold-core structure (up to 500 mb) of
cloud clusters has been observed and previously discussed by
Riehl (1948, 1954, 1969). The pre-typhoon cluster, on the other hand,
is weakly warm-core at 600-800 mb. Intensifying and mature tropical
cyclones are strongly warm-core at these levels. Hubert (1955) and
Yanai (1961a, 1961b) have presented case studies in which a pre-existing
disturbance transformed from a cold-core to a warm-core disturbance
in the middle troposphere (500-800 mb). On the other hand, the com-
posited data in the earliest pre-typhoon stages indicate a slightly
warm-core structure. Undoubtedly, it is possible that the transformation
from cold-core to warm-core took place in some cases just before the
cluster's position was identified for this study. It is also possible
that the ITCZ pre-typhoon clusters may form initially in strong ITCZ's
which already possess a warm-core structure. The maximum winds in the
ITCZ are typically in the lower as opposed to the middle troposphere.

In either case, one of the first indications that a tropical weather system may become a tropical cyclone is the presence of a warm-core structure in the 600-800 mb layer. It should be emphasized that the level of maximum tangential circulation is a good indicator of the thermal structure. An ITCZ disturbance with a maximum circulation at 500-600 mb poses no threat of becoming a tropical cyclone until that characteristic disappears. Conversely, an ITCZ disturbance with a maximum circulation at 800-950 mb will often become a tropical cyclone. For prediction purposes it is of interest to note that the favorable genesis characteristic may often be present several days before any significant intensification occurs.

6.3 Relative Vorticity

This investigation has identified the greater low-level relative vorticity of pre-typhoon clusters. Yanai (1961a) identified a deep, broad-scale vorticity convergence as an important initial requirement for tropical cyclone formation. A low-level (or doldrum) trough condition which is characterized by a sharper north-south zonal shearing flow than normal is most favorable for genesis. A strengthening of the monsoon trough in the lower levels results in increased low-level vorticity and warm-core structure.

In the middle troposphere non-developing and pre-typhoon clusters have very similar relative vorticity. However, in the upper troposphere where relative vorticity is negative, there are significant differences. The pre-typhoon clusters have significantly more negative relative vorticity both within the cluster and in its surrounding region.

Riehl (1948) viewed tropical cyclone genesis as a result of the proper superposition of upper tropospheric systems and waves in the

low-level easterlies. There could be in his scheme relative motion
between the upper and lower level systems. Several studies (Alaka,
1962; Fett, 1966; Colón and Nightingale, 1963; and Sadler, 1967a, 1967b,
1974) stress cyclone formation as it relates to particular patterns
in the upper troposphere. The composited data of this study supports
these findings to the extent that significant differences in mean
relative vorticity between pre-typhoon and non-developing clusters
in the upper troposphere are noted. However, specific transient wind and
height patterns such as a trough in the westerlies cannot easily be iden-
tified with composited data.

7. SUMMARY

Several major facts about ITCZ pre-typhoon cloud clusters have been established by this investigation. Many of these reinforce the findings and conclusions of previous studies.

1) Pre-typhoon cloud clusters are located in regions with mean low-level relative vorticity in the vicinity of the cluster approximately twice as large as that observed with non-developing cloud clusters.

2) The mean vertical motion is about 25% greater with pre-typhoon clusters than with non-developing clusters when measured within a large (8° diameter) region centered on the clusters.

3) The cold-core structure in the 500-800 mb layer, characteristic of non-developing cloud clusters, is not present with pre-typhoon cloud clusters. This feature is further substantiated by the tangential wind and relative vorticity data. The pre-typhoon clusters have a vorticity maximum just above the boundary layer as opposed to a maximum in the middle troposphere with non-developing cloud clusters.

4) In the mean, non-developing clusters exist in regions with larger vertical shear of the mean zonal wind. As a result, the ventilation integrated through the troposphere is greater with non-developing clusters than with pre-typhoon clusters. This inhibits some of the sensible and latent heat accumulation which is favorable for tropical cyclone formation.

5) The outflow in the 150-250 mb layer is more anticyclonic with pre-typhoon cloud clusters than with non-developing clusters. The resultant greater export of negative relative angular momentum has the net effect of importing more positive momentum. This feature, in addition to the differences in low-level relative vorticity, allows significantly greater magnitudes of relative angular momentum to be imported into the pre-typhoon cluster region compared with the non-developing cluster.

6) Mean lapse rates and potential buoyancy are very similar for both classes of systems.

It should be stressed that all of the above differences between pre-typhoon and non-developing cloud clusters were noted at a time well before any significant intensification of the pre-typhoon cluster. The

74

observed surface wind speeds averaged less than 5 m/sec in the immediate area of both the non-developing cluster and the pre-typhoon cluster.

8. THE ROLE OF FRICTIONAL CONVERGENCE IN TROPICAL CYCLONE GENESIS

BY William M. Gray and John McBride

8.1 Numerical Modeling of Tropical Cyclone Formation

The aspect of typhoon formation which is least understood is that of how the weak precursor cyclone extending through most of the troposphere (with vorticity $\sim$ 50-100 x 10^{-6} sec^{-1}) is formed from a weak open-wave disturbance with initial low level vorticity of only 10-15 x 10^{-6} sec^{-1}. This very early stage in the typhoon formation process is termed 'cyclone genesis'. By contrast, the question of 'cyclone intensification' or growth of an already formed deep tropospheric cyclone is much better understood.

Following the initial studies of Charney and Eliassen (1964) and Kuo (1965), several numerical modelers have simulated the intensification process of an already specified tropical cyclone which extends through the depth of the troposphere. These modeling efforts have been primarily directed towards obtaining realistic simulations of tropical cyclone growth rates from existing cyclones whose inner 100-200 km radius vorticity is of an order of magnitude larger than that of the typical pre-cyclone disturbance dealt with in the current study. In Table 10 the strengths of the circulations from which typhoons develop are shown. This is compared with Table 11 which shows the initial cyclone strengths assumed by modelers.

The cyclone models are based on the theory of Conditional Instability of the Second Kind first formulated by Charney and Eliassen (1964) and Ooyama (1964). The CISK theory is one of self-amplification of the disturbance through the mechanism of boundary layer convergence being compensated by upward pumping of moist air. This results in the release

TABLE 10

Tangential Wind vs. Radius and Relative Vorticity for
Various Stages of Tropical Cyclone Intensification

Data	Maximum Tangential Wind (900 mb or top of PBL) $(m\ sec^{-1})$	Radius of Maximum Tangential Wind (km)	Mean Relative Vorticity Inside the Radius of Maximum Tangential Wind $(10^{-6}sec^{-1})$
Non-developing cluster (Stage 00)	1.6	$\sim$ 400	8
Non-developing cluster (Stage 0)	2.5	$\sim$ 500	10
Pre-typhoon cluster (Stage 2)	5.3	$\sim$ 400	26
Intensifying Tropical Depression (Stage 4)	10.1	$\sim$ 200	100
Mean assumed Initial vortex of modelers[*]	12.2	172	142

[*]Based on the numerical models listed in Table 11, excluding Carrier,
(1971).

of latent heat, a consequent fall in surface pressure and enhancement
of the surface convergence.

The theory explains well the intensification of an already developed
cyclone. Cyclones of the strengths and vertical depths initially assumed by most modelers, however, are rare. About two-thirds of all
cyclones of such intensity reach typhoon strength. The processes
responsible for formation of the initial cyclone from which the modelers
start their integrations have yet to be elucidated.

Table 11

Summary of Recent Numerical Modeling Papers on Hurricane Development
and Their Assumed Initial Cyclone Strengths

Modelers	Assumed Initial Maximum Wind Velocity and Radius of Maximum Wind		Vortex Vorticity Inside the Radius of Maximum Winds (10^{-6}sec^{-1})	Type of Vortex
Kuo (1965)	10 m/sec,	141 km	142	Symmetrical
Yamasaki (1968)	4.7m/sec,	100 km	94	Symmetrical
Ooyama (1969)	10 m/sec,	50 km	400	Symmetrical
Miller (1969)	10 m/sec,	200 km	100	Real Vortex
Rosenthal (1970)	7 m/sec,	250 km	56	Symmetrical
Sundquist (1970)	15 m/sec,	200 km	150	Symmetrical
Carrier (1971)	21 m/sec,	50 km	840	Symmetrical
Anthes, et al. (1971a,1971b)	18 m/sec,	240 km	150	A-symmetrical
Anthes (1972)	18 m/sec,	240 km	150	A-symmetrical
Mathur (1972)	15 m/sec,	200 km	150	A-symmetrical
Harrison (1973)	∿10 m/sec,	∿120*km	∿170	A-symmetrical
Kurihara and Tuleya (1974)	12 m/sec,	200 km	120	Symmetrical
Ceselski (1974)	17 m/sec,	∿100-150 km	∿200	Real Vortex

Typical pre-cyclone cloud cluster ∿10-15

---

*Estimated from initial height field

8.2 Frictional Induced Boundary Layer Convergence

Figure 37 shows the vertical profiles of divergence for the non-developing clusters and for all stages of typhoon development. The deep inflow up through 400 mb in the early stages means that in these stages, only a small fraction of the mass converging into the cluster is frictionally forced. This observation is made quantitative by the following simple calculation of the magnitude of the frictionally induced convergence.

Gray (1972) and Gray and Mendenhall (1974) statistically analyzed pibal and rawinsonde wind data over the tropical oceans. They showed that, after the thermal wind effect had been eliminated from the data, the typical veering of the surface wind relative to the wind at the top of the boundary layer is about 12°. It is assumed that this veering is due to mechanical frictional processes. (It is emphasized that the veering angle referred to is that between the surface wind and the wind at the top of the layer of frictional influence. It is not the angle between the surface wind and the surface isobars. In the tropics the latter angle may be much larger.)

Gray (1972) observed also that over the tropical oceans the decrease of wind speed with depth in the boundary layer is small. This is demonstrated in Fig. 38.

In Fig. 39 a schematic of the wind at the top of the boundary layer at a distance R from the center of the cluster is shown. From the figure it is seen that the convergence at the top of the boundary layer is equal to tan β times the vorticity. If it is assumed that the tangential wind maintains its strength through the boundary layer, and that the PBL frictional processes bring about a further 12° turning
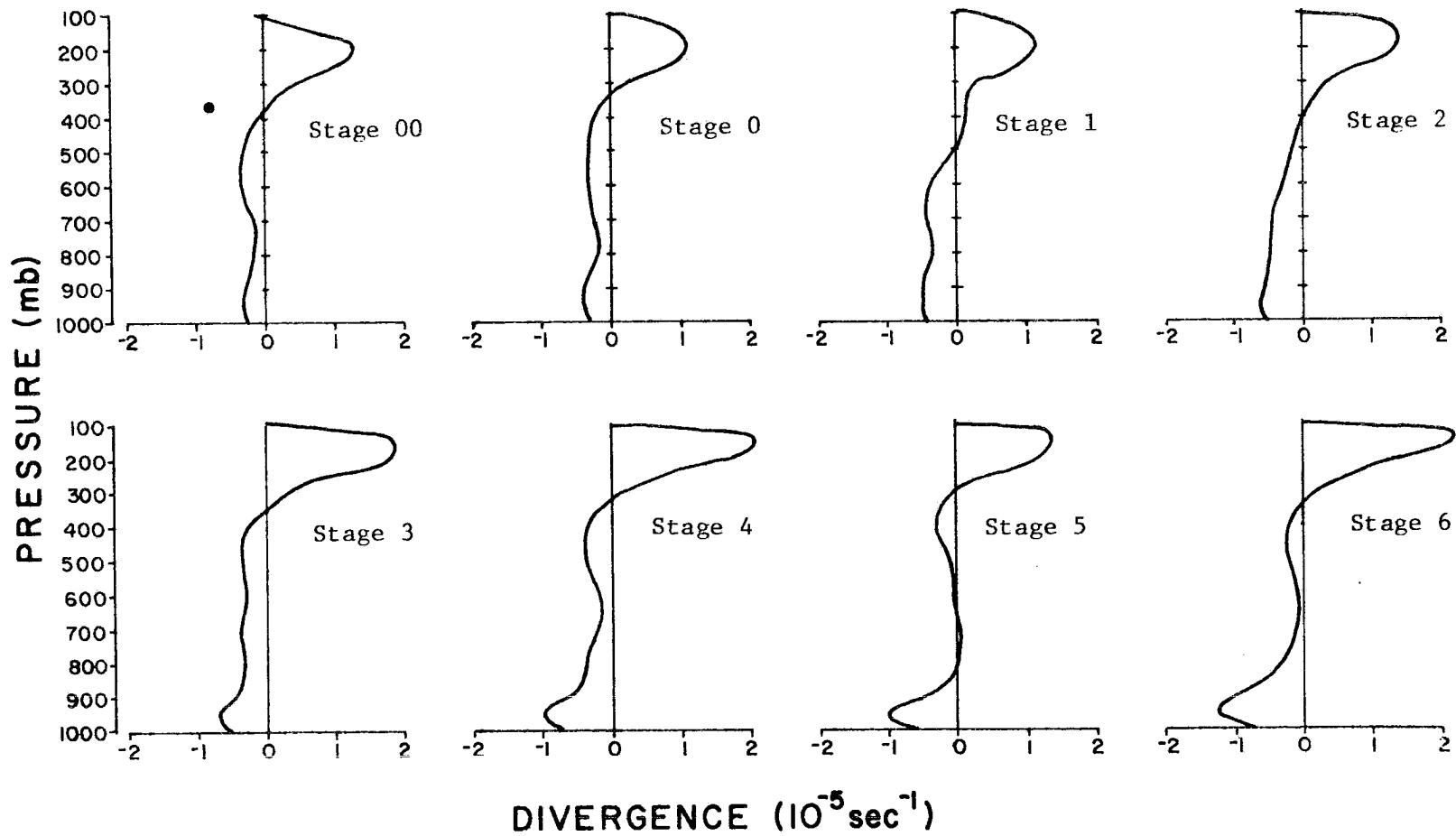
Fig. 37. Mean divergence within the r = 0-4° area for all data sets.
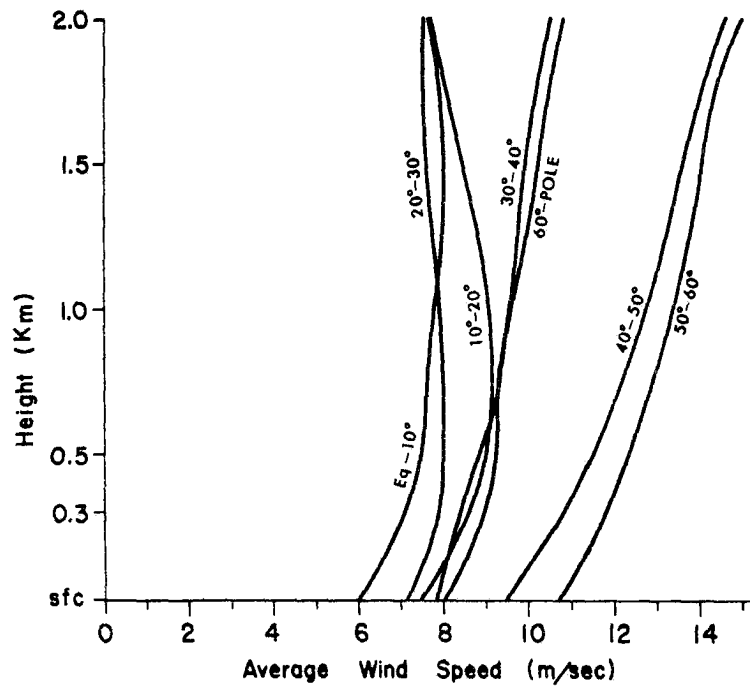
Fig. 38. Variation of wind speed in the lowest 2 km - from Gray (1972).
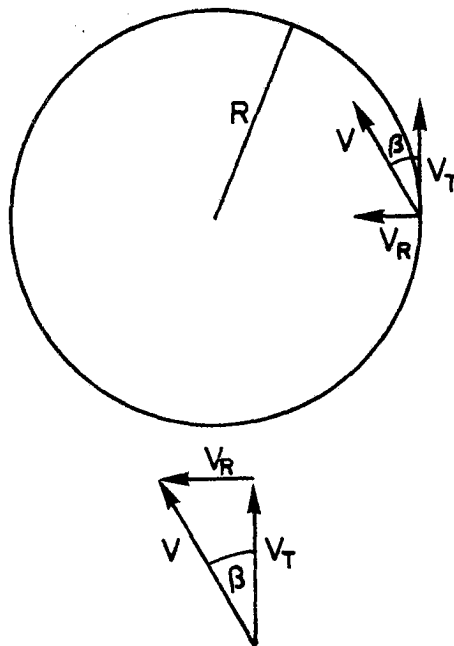
V= Wind at top of Planetary
   Boundary Layer (P.B.L.)

β = Inflow angle at top of P.B.L.

V_T = Tangential wind = $V\cos\beta$

V_R = Radial wind = $V\sin\beta$

Fig. 39. Schematic depiction of the wind field at the top of the
boundary layer at the radius R. By Stokes' theorem, the
vorticity averaged over the circle = $2\ V_T/R = \overline{\zeta_T}$. By Gauss'
theorem, the convergence averaged over the circle
= $2\ V_R/R = \tan\beta \cdot 2\ V_T/R = \tan\beta \cdot \overline{\zeta_T}$.

of the wind, then the convergence at the surface is equal to tan

$(\beta + 12^{\circ}) \cdot \zeta_T$. Thus, if the veering varies linearly with height,

the average convergence in the boundary layer is $\frac{1}{2}\overline{\zeta_T}$ (tan β + tan (β +

12°)). Defining C_F as the additional convergence due to the frictional

turning of the wind:

C_F = calculated boundary layer - convergence at the top of the
convergence boundary layer

$$C_F = \frac{1}{2}\overline{\zeta_T} \text{ (tan } \beta + \text{ tan } (\beta + 12^{\circ}))- \overline{\zeta_T} \text{ tan } \beta$$

$$\approx \frac{1}{2}\overline{\zeta_T} \text{ tan } 12^{\circ}$$

$$C_F \approx 1/10 \ \overline{\zeta_T} \tag{1}$$

Equation (1) is only approximate. More detailed calculations in-

volving assumed wind speed profiles and veering angle profiles have

shown, however, that the approximation is quite good.

Assuming that the planetary boundary layer extends to 850 mb,

Table 12 was constructed using equation (1) and the measured convergences

shown in Fig. 37.

From the table it is seen that frictional convergence, as here

defined C_F, is not the dominant mechanism importing mass into the develop-

ing tropical cyclone. C_F makes up only 40% of the observed surface to

850 mb mass convergence for both the pre-typhoon and the non-developing

cluster data sets. From the intensifying tropical storm stage (stage 4)

onwards, C_F accounts for 70% of the total boundary layer convergence.

At this stage the boundary layer convergence accounts for $\frac{1}{2}$ of the total

mass inflow.

TABLE 12

Observed mass convergence and calculated frictional convergence in gm/cm^2 day^{-1} for different stages of typhoon formation.

CONVERGENCE 0 to $4°$ (gm/cm^2 day^{-1})

Data	(1) Observed Convergence sfc to 300 mb	(2) Observed Convergence sfc to 850 mb	(3) $1/10\bar{\zeta}_T$	(4) $\dfrac{1/10\bar{\zeta}_T}{\text{Observed sfc-850}}$	(5) $\dfrac{1/10\bar{\zeta}_T}{\text{Observed sfc-300}}$	(6) $\dfrac{\text{Observed sfc-850}}{\text{Observed sfc-300}}$
Stage 00	105	30	11	.4	.1	.3
Stage 0	115	30	12	.4	.1	.3
Stage 1	140	65	25	.4	.2	.4
Stage 2	180	75	33	.4	.2	.4
Stage 3	200	75	47	.6	.2	.4
Stage 4	200	90	59	.7	.3	.5
Stage 5	125	90	62	.7	.5	.7
Stage 6	215	130	89	.7	.4	.6

The first column is the total observed convergence to 300 mb

The second column is the observed convergence from the surface to 850 mb

The third column is the calculated convergence due to frictional veering = C_F

The fourth column is the ratio of C_F to the actual boundary layer convergence

The fifth column is the ratio of C_F to the total convergence

The sixth column is the ratio of the observed boundary layer convergence to the total convergence

83

It should be noted from the last column of the table that in
all stages of development there is a large amount of down gradient flow
above the boundary layer. Even in the stage 6 (typhoon) data set 40%
of the mass inflow occurs above 850 millibars.

8.3 Role of Radiation in the Maintenance of Tropical Weather Systems

The primary energy source for tropical storms is the release of
latent heat. The magnitude of the sensible temperature warming associa-
ted with latent heat release in a weaker system such as the pre-typhoon
cluster, however, is very small. The condensation energy release is
directly tied to upward vertical motion. It typically does not bring
about direct environmental sensible temperature gains but goes primarily
into potential energy gains (Gray, 1973). The troposphere experiences
warming due to condensation only as a consequence of compensating dry
adiabatic sinking motion (Lopez, 1973). Much of this compensating sink-
ing motion occurs at locations removed from the cloud areas. The sub-
sidence warming occurring within the tropical disturbance is largely
expended in balancing the cloud region liquid water reevaporation due
to cloud detrainment. Williams and Gray (1973) and Ruprecht and Gray
(1976) have demonstrated that the direct influence of the typical 4-5°
diameter cluster condensation (equivalent to 1000-1500 calories/cm^2 per
day) on cluster sensible temperature change is nearly zero. Thus, it
is unlikely that condensation energy gain is the primary source of the
pressure gradients associated with the inflow at all levels from the
surface to 400 millibars.

In section 5 it was shown that the ventilation or movement of air
through the cluster is small ($\sim$ 1 m/sec in the lower and middle tropo-
sphere for the Stage 2 cluster). In addition, horizontal relative

vorticity gradients are small. Thus it is felt that vorticity advection cannot be the primary cause of the observed divergence profile.

Jacobson and Gray (1976) proposed that the deep tropospheric convergence is maintained by the differences in the radiative cooling profiles of the thick cirrus-shield covered cluster and the surrounding clear area. Using composited rawinsonde data and rainfall data from tropical Pacific atolls and small islands, they demonstrated that both the cluster convergence and the associated rainfall undergo a significant diurnal variation. The phase and magnitude of the variation agree well with that expected from radiational forcing.

As shown in Fig. 37, the deep convergence is maintained through all stages of cyclone formation. If the system – versus – environment radiation differences are fundamental to the maintenance of this convergence profile, this source of available potential energy must be incorporated into future theoretical and modelling studies of cyclone genesis.

8.4 Summary

Although it is believed that cloud-cluster vs. cloud-cluster environment radiation differences are fundamental to tropical disturbance structure-maintenance and cyclone genesis, these relative radiation influences by themselves will probably not well distinguish (because of similar cloud cluster cirrus shields) between intensifying and non-intensifying systems. Differences in ventilation, low-level vorticity, outflow, etc. (as have been shown) are likely to be the major cluster genesis distinguishing features and not radiation. Of course, relative radiation differences cannot be used to explain cluster initiation.

Here the more mechanical mechanisms of baro-tropic baroclinic instability,
etc. or other more purely dynamical processes must be responsible. It
is likely that frictional effects are important in this pre-cluster stage.
Nevertheless, relative radiational differences should be important to
the realistic modeling of cloud cluster maintenance and of cyclone genesis.
Pre-cyclone disturbances typically exist for 2-4 days in a dormant pre-
intensification stage. These systems probably could not maintain their
deep inflow patterns during this long a period against the inhibiting
influences of horizontal temperature-moisture ventilation, divergence,
etc. unless cluster and surrounding radiation differences were not con-
tinually acting to maintain the system's deep transverse circulation.
It is predicted that realistic future numerical modeling of the cloud
cluster will require that these radiational influences be included. How
can the cyclone genesis process be correctly modeled if the deep inflow
of the precursor system is not also properly incorporated?

ACKNOWLEDGEMENTS

BIBLIOGRAPHY

Alaka, M. A., 1962: On the occurrence of dynamic instability in incipient and developing hurricanes. Mon. Wea. Rev., 2, 49-58.

Anthes, R. A., 1972: Development of asymmetries in a three-dimensional numerical model of the tropical cyclone. Mon. Wea. Rev., 100, 461-476.

Anthes, R. A., S. L. Rosenthal, and J. W. Trout, 1971a: Preliminary results from an asymmetric model of the tropical cyclone. Mon. Wea. Rev., 99, 744-758.

Anthes, R. A., J. W. Trout, and S. L. Rosenthal, 1971b: Comparisons of tropical cyclone simulations with and without the assumption of circular symmetry. Mon. Wea. Rev., 99, 759-766.

Arnold, C. A., 1977: Forthcoming CSU report on tropical cyclone convection using DMSP satellite data.

Carrier, G. F., 1971: The intensification of hurricanes. J. Fluid Mech., 49, 145-158.

Ceselski, B. F., 1974: Cumulus convection in weak and strong tropical disturbances. J. Atmos. Sci., 31, 1241-1255.

Chang, C. P., 1970: Westward propagating cloud patterns in the tropical Pacific as seen from time-composite satellite photographs. J. Atmos. Sci., 27, 133-138.

Charney, J. C. and A. Eliassen, 1964: On the growth of the hurricane depression. J. Atmos. Sci., 21, 68-75.

Colón, J. A. and W. R. Nightingale, 1963: Development of tropical cyclones in relation to circulation patterns at 200 mb level. Mon. Wea. Rev., 91, 329-336.

Dunn, G. E., 1940: Cyclogenesis in the tropical Atlantic. Bull. Am. Meteor. Soc., 21, 215-229.

Erickson, S., 1977: Forthcoming CSU report on tropical cyclone genesis using DMSP satellite data.

Fett, R. W., 1966: Upper-level structure of the formative tropical cyclone. Mon. Wea. Rev., 1, 9-18.

Fett, R. W., 1968: Typhoon formation within the zone of the intertropical convergence. Mon. Wea. Rev., 96, 106-117.

Frank, W. M., 1976: The structure and energetics of the tropical cyclone. Colo. State Univ., Atmos. Sci. Paper No. 258, Ft. Collins, CO, 180 pp.

George, J. and W. M. Gray, 1976: Tropical cyclone recurvature and non-recurvature as related to surrounding wind-height fields. J. Appl. Meteor., January issue.

George, J. and W. M. Gray, 1977: Tropical cyclone motion and surrounding parameter relationships. J. Appl. Meteor., January issue.

Gray, W. M., 1968: Global view of the origin of tropical disturbances and storms. Mon. Wea. Rev., 96, 669-770.

Gray, W. M., 1972: A diagnostic study of the planetary boundary layer over the oceans. Colo. State Univ., Atmos. Sci. Paper No. 179, Ft. Collins, CO, 95 pp.

Gray, W. M., 1973: Cumulus convection and large-scale circulations, Part I: Broadscale and meso-scale interactions. Mon. Wea. Rev., 101, 839-855.

Gray, W. M., 1975: Tropical cyclone genesis. Colo. State Univ., Atmos. Sci. Paper No. 243, Fort Collins, CO, 121 pp.

Gray, W. M. and B. Mendenhall, 1974: A statistical analysis of factors influencing the wind veering in the planetary boundary layer. Climatological Research, The Hermann Flohn 60th Anniversary Vol., 167-194.

Harrison, E. J., 1973: Three-dimensional numerical simulations of tropical storms utilizing nested finite grids. J. Atmos. Sci., 30, 1528-1543.

Hubert, L. F., 1955: A case study of hurricane formation. J. Meteor. 12, 486-492.

Jacobson, R. W., Jr. and W. M. Gray, 1976: Diurnal variation of oceanic deep cumulus convection, Paper I: Observational evidence, Paper II: Physical hypothesis. Colo. State Univ., Atmos. Sci. Paper No. 243, Fort Collins, CO, 106 pp.

Kuo, H. L., 1965: On formation and intensification of tropical cyclones through latent heat release by cumulus convection. J. Atmos. Sci. 22, 40-63.

Kurihara, Y., and R. E. Tuleya, 1974: Structure of a tropical cyclone developed in a three-dimensional numerical simulation model. J. Atmos. Sci., 31, 893-919.

Lopez, R. F., 1968: Investigation of the importance of cumulus convection and ventilation in early tropical storm development. Colo. State Univ., Atmos. Sci. Paper No. 124, Fort Collins, CO, 86 pp.

Lopez, R. F., 1973: Cumulus convection and larger scale circulations. Part II: Cumulus and mesoscale interactions. Mon. Wea. Rev., 101, 856-870 pp.

Mathur, M. B., 1972: Simulation of an asymmetric hurricane with a fine
    mesh multiple grid primitive equation model. Ph.D. dissertation,
    Florida State University, Tallahassee, Florida, 162 pp.

Miller, B. I., 1969: Experiment in forecasting hurricane development with
    real data. ESSA Tech. Memorandum ERLTM-NHRL 85, Miami, Fla. 23 pp.

Nitta, T. and M. Yanai, 1969: A note of the barotropic instability of
    the tropical easterly current. J. Meteor. Soc. Japan, 47, 127-130.

Ooyama, K., 1964: A dynamical model for the study of tropical cyclone
    development. Geofis. Intern., 4 187-198.

Ooyama, K., 1969: Numerical simulation of the life cycle of tropical
    cyclones. J. Atmos. Sci., 26, 3-40.

Palmén, E. H., 1948: On the formation and structure of tropical cyclones.
    Geophysica, Helsinki, 3, 26-38.

Reed, R. J. and E. E. Recker, 1971: Structure and properties of synoptic-
    scale wave disturbances in the equatorial western Pacific. J. Atmos.
    Sci., 28, 1117-1133.

Riehl, J., 1948: On the formation of typhoons. J. Meteor., 5, 247-264.

Riehl, H., 1950: A model of hurricane formation. J. Appl. Physics, 9,
    917-925.

Riehl, H., 1954: Tropical Meteorology. McGraw-Hill, New York, 392 pp.

Riehl, H.. 1969: Some aspects of cumulonimbus convection in relation
    to tropical weather disturbances. Bull. Amer. Meteor. Soc., 50,
    587-595.

Rosenthal, S. L., 1970: A circularly symmetric primitive equation of
    tropical cyclone development containing an explicit water vapor
    cycle. Mon. Wea. Rev., 98, 643-663.

Ruprecht, E. and W. M. Gray, 1976: Analysis of satellite-observed tropical
    cloud clusters. Papers I and II. Tellus, 28, 391-425.

Sadler, J. C., 1967a: On the origin of tropical vortices. Working
    Panel on Trop. Dyn. Meteor. Naval Post Graduate School, Monterey,
    CA, 39-75.

Sadler, J. C., 1967b: The tropical tropospheric trough as a secondary
    source of typhoons and a primary source of tradewind disturbances.
    Final Rept. Cont. AF19 (628)3860, A. F. Cambridge Res. Lab., Bedford,
    MA., Rept. 67-12, 44 pp.

Sadler, J. C., 1974: A role of the tropical upper tropospheric trough in
    early seasonal typhoon development. Tech. Paper No. 9-74, U.S.
    Navy Environmental Prediction Research Facility Report. 54 pp.

Sartor, J., 1968: Monthly climatological wind fields associated with tropical storm genesis in the West Indies. Colo. State Univ., Atmos. Sci. Paper, Fort Collins, CO, 34 pp.

Shapiro, L., 1975: Tropical waves and tropical cyclone generation. Unpublished Ph.D. Thesis, Harvard Univ., 270 pp.

Sundquist, H., 1970: Numerical simulation of the development of tropical cyclones with a ten-layer model. Part I. Tellus, 22, 359-390.

Wachtmann, R. F., 1968: Role of angular momentum transport in tropical storm dissipation over tropical oceans. Colo. State Univ., Atmos. Sci. Paper, Fort Collins, CO, 46 pp.

Wallace, J. M., 1970: Time-longitude sections of tropical cloudiness (December 1966-November 1967). ESSA Technical Report, NESC 56, National Environmental Satellite Center, Suitland, MD, 37 pp.

Williams, K. T., and W. M. Gray, 1973: A statistical analysis of satellite-observed trade wind cloud clusters in the western north Pacific. Tellus, 21, 323-336.

Yamasaki, M., 1968: Numerical simulation of tropical cyclone development with the use of primitive equations. J. Meteor. Soc. Jap., 46, 178-201.

Yanai, M., 1961a: A detailed analysis of typhoon formation. J. Meteor. Soc. Japan, 39, 187-214.

Yanai, M., 1961b: Dynamical aspects of typhoon formation. J. Meteor. Soc. Japan, 39, 282-309.

Yanai, 1964: Formation of tropical cyclones. Reviews Geophys., 2, 367-414.

Author: Raymond Zehr

TROPICAL DISTURBANCE INTENSIFICATION

Subject Headings:

Tropical cyclone genesis
Tropical cloud clusters

An observational study of tropical cyclone genesis was made by compositing western Pacific rawinsonde data with respect to both pre-typhoon and non-developing cloud clusters. The size, intensity, and mean vertical motion of the disturbances which eventually evolved into typhoons were similar to the non-developing clusters which did not intensify. However, four primary physical differences between pre-typhoon and non-developing clusters are found: 1) The low-level relative vorticity with the pre-typhoon clusters was about twice as large. 2) The non-developing clusters were cold-core in the 500-800 mb layers while the pre-typhoon clusters were slightly warm-core at these levels. 3) The ventilation (non-divergent flow through the cluster area) which advects heat energy away from the cluster was larger with the non-developing clusters in the warm-core layers (200-500 mb) and ventilation of moisture out of the non-developing clusters was significantly larger at lower tropospheric levels (500-900 mb). 4) The outflow in the upper troposphere was similar in magnitude but markedly more anticyclonic with the pre-typhoon clusters.

Boundary layer (surface-900 mb) frictional convergence accounts for only a small fraction of the net mass convergence into the pre-typhoon cloud cluster which typically extends up to 300-400 mb. The percentage of boundary layer convergence to total convergence does, however, increase as the intensification process proceeds. Other physical mechanisms such as cloud cluster minus surrounding radiational differences must likely be hypothesized to explain the cloud cluster's deep-layer inflow in its early stages of existence and intensification.